



Scholars Research Library

Der Pharma Chemica, 2015, 7(2):243-269
(<http://derpharmachemica.com/archive.html>)



ISSN 0975-413X
CODEN (USA): PCHHAX

A DFT and Docking study of the relationships between electronic structure and 5-HT_{2B} receptor binding affinity in N-benzylphenethylamines

Juan S. Gómez-Jeria* and Andrés Robles-Navarro

Quantum Pharmacology Unit, Department of Chemistry, Faculty of Sciences, University of Chile, Las Palmeras, Santiago, Chile

ABSTRACT

An extensive study was carried out to find formal relationships between electronic structure and 5-HT_{2B} receptor binding affinity in a family of 44 N-benzylphenethylamines. These molecules were also docked to a structure of the human 5-HT_{2B} receptor. The QSAR results were able to detect several atoms involved in the binding with HT_{2B} receptor but failed at least in one important case. Docking results show that some molecules experience strong intramolecular π - π interactions producing folded structures. A given moiety of the molecules is able to interact with more than one residue of the receptor. Not always a certain moiety interacts with the same residue. The necessity of finding a more exact relationship between quantum-chemical and docking results needs a revision of the common skeleton concept.

Keywords: 5-HT_{2B} receptor, QSAR, DFT, serotonin, binding affinity, docking, N-benzylphenethylamines.

INTRODUCTION

The serotonergic system is one of the oldest evolutionary neurotransmitter systems [1, 2]. The center of this system is serotonin (5-hydroxytryptamine, 5-HT, β -aminoethyl-5-hydroxyindole), a molecule synthesized by the human body from the amino acid L-tryptophan. It is metabolized via monoamine oxidase to 5-hydroxyindolaldehyde and finally to 5-hydroxyindolacetic acid (via aldehydedehydrogenase). *Mammals use 5-HT as a neurotransmitter within the central and peripheral nervous systems, and also as a local hormone in numerous other tissues, including the gastrointestinal tract, the cardiovascular system and immune cells* [3]. 5-HT exerts its effects by interacting with at least 14 subtypes of receptors. Among them the 5-HT_{2B} receptor, a member of the 5-HT₂ receptor subfamily, is lightly expressed in discrete sub regions of the central nervous system and greatly expressed in the fundus of the stomach, heart, kidney and liver. The physiological role of 5-HT_{2B} receptors is still uncertain but they have been implicated in anxiety, cardiac function, depression, inhibition of liver regeneration, migraine, morphogenesis, pulmonary vasoconstriction and sleep disorder [4-34]. 5-HT_{2B} receptors are overexpressed in human failing heart. The 5-HT_{2B} receptor stimulation can lead to pathological proliferation of cardiac valves fibroblasts, which with chronic overstimulation of 5-HT_{2B} can lead to a severe valvulopathy. 5-HT_{2B} receptors have also been implicated in drug-induced valvular heart disease [8, 11, 28, 35-39]. For these reasons, the most recent research has focused on the possible application of 5-HT_{2B} antagonists as a treatment for chronic heart disease. Several families of molecules that bind to 5-HT_{2B} receptor have been synthesized [4, 40-52]. In one case, the 5-HT_{2B} receptor binding affinity was determined for a large group of N-benzylphenethylamines [47]. Recently, the crystal structure of the human 5-HT_{2B} receptor bound to ergotamine was determined [53]. As a contribution for a better knowledge of the 5-HT_{2B}-ligand interactions we present here the results of a study of the formal relationships between electronic structure and 5-HT_{2B} receptor binding affinity for a set of 44 molecules. Also, a second study was performed by docking all these molecules to the 5-HT_{2B} receptor.

MATERIALS AND METHODS

The method

The model-based method [54] relating drug-receptor equilibrium constants with molecular structure has been described in great detail elsewhere [55-59]. Here we shall present, in a standard formulation used in most of our papers, the final results. The drug-receptor affinity constant, $\log(K_i)$ (or $\log(IC_{50})$, pK, etc.), is a linear function having the following form:

$$\begin{aligned}
 pK_i = & a + bM_{D_i} + \sum_j \left[e_j Q_j + f_j S_j^E + s_j S_j^N \right] + \\
 & + \sum_j \sum_m \left[h_j(m) F_j(m) + x_j(m) S_j^E(m) \right] + \sum_j \sum_{m'} \left[r_j(m') F_j(m') + t_j(m') S_j^N(m') \right] + \\
 & + \sum_j \left[g_j \mu_j + k_j \eta_j + o_j \omega_j + z_j \zeta_j + w_j Q_j^{\max} \right]
 \end{aligned}
 \tag{1}$$

where M is the drug's mass, Q_j is the net charge of atom j , S_j^E and S_j^N are, respectively, the total atomic electrophilic and nucleophilic superdelocalizabilities of Fukui *et al.*, $F_{j,m}$ ($F_{j,m'}$) is the Fukui index of the occupied (empty) MO m (m') located on atom j . $S_j^E(m)$ is the atomic electrophilic superdelocalizability of MO m on atom j , etc. The total atomic electrophilic superdelocalizability of atom j corresponds to the sum over occupied MOs of the $S_j^E(m)$'s and the total atomic nucleophilic superdelocalizability of atom j is the sum over empty MOs of the $S_j^N(m)$'s [60]. The last bracket of the right side of Eq. 1 contains a new set of local atomic reactivity indices obtained directly from the Hartree-Fock LCAO-MO and Density Functional theories [56, 58, 59]. Below, HOMO $_j^*$ refers to the highest occupied molecular orbital localized on atom j and LUMO $_j^*$ to the lowest empty MO localized on atom j . They are called the local atomic frontier MOs. The molecule's MOs do not carry an *. μ_j is the local atomic electronic chemical potential of atom j (the HOMO $_j^*$ -LUMO $_j^*$ midpoint), η_j is the local atomic hardness of atom j (the HOMO $_j^*$ -LUMO $_j^*$ gap), ω_j is the local atomic electrophilicity of atom j , ζ_j is the local atomic softness of atom j and Q_j^{\max} is the maximal amount of electronic charge that atom j may accept from another site. The application of this method to the drug-receptor interaction has been very successful [61-87]. The extension of this method to any kind of biological activities opened a totally new area of research [88-101].

Selection of molecules and experimental data.

The selected molecules are a group of 44 *N*-Benzylphenethylamines derivatives with affinity for the 5-HT $_{2B}$ cloned human receptors [47]. [3 H]-LSD was employed as radioligand for displacement measurements. The selected molecules and their 5-HT $_{2B}$ binding affinities ($pK = -\log(K)$) are shown in Figure 1 and Table 1.

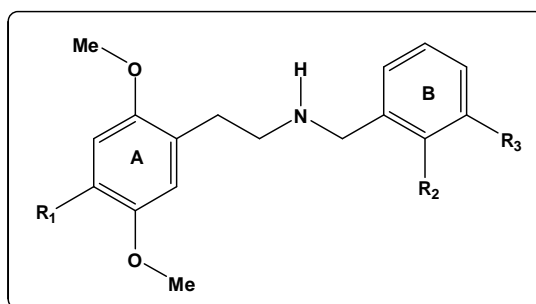


Figure 1. General formula of *N*-Benzylphenethylamines

Table 1. N-Benzylphenethylamines and 5-HT_{2B} binding affinity [47]

Mol.	R ₁	R ₂	R ₃	pK _{5-HT_{2B}}	Mol.	R ₁	R ₂	R ₃	pK _{5-HT_{2B}}
1	Br	OMe	H	9.3	23	Pr	F	H	8.78
2	Br	OH	H	8.1	24	Pr	O-CH ₂ -O	H	8.24
3	Br	F	H	8.23	25	SMe	OMe	H	9.04
4	Br	O-CH ₂ -O	H	8.85	26	SMe	OH	H	8.8
5	Cl	OMe	H	8.95	27	SMe	F	H	7.84
6	Cl	OH	H	8.08	28	SMe	O-CH ₂ -O	H	8.61
7	Cl	F	H	7.57	29	SEt	OMe	H	9.07
8	Cl	O-CH ₂ -O	H	8.80	30	SEt	OH	H	8.71
9	F	OMe	H	8.12	31	SEt	F	H	8.09
10	F	OH	H	7.68	32	SEt	O-CH ₂ -O	H	8.75
11	F	F	H	7.11	33	SPr	OMe	H	8.64
12	F	O-CH ₂ -O	H	7.47	34	SPr	OH	H	8.41
13	Me	OMe	H	8.41	35	SPr	F	H	7.86
14	Me	OH	H	7.96	36	SPr	O-CH ₂ -O	H	8.16
15	Me	F	H	7.3	37	CF ₃	OMe	H	8.96
16	Me	O-CH ₂ -O	H	7.92	38	CF ₃	OH	H	8.46
17	Et	OMe	H	8.67	39	CF ₃	F	H	7.8
18	Et	OH	H	8.65	40	CF ₃	O-CH ₂ -O	H	8.34
19	Et	F	H	7.7	41	CN	OMe	H	7.68
20	Et	O-CH ₂ -O	H	8.4	42	CN	OH	H	7.21
21	Pr	OMe	H	7.7	43	CN	F	H	6.41
22	Pr	OH	H	8.34	44	CN	O-CH ₂ -O	H	7

To gain more information about the drug-receptor interaction we have considered three different groupings of molecules: the whole set (n=43, called set I), a second set in which the R₁ substituent is an alkyl moiety (molecules 13-24 and 37-40, n=16, called set II) and a third set in which R₁ is halogen, S-alkyl or CN (molecules 1-12, 26-36 and 42-44, n=27, called set III). The common skeleton for all sets is shown in Fig. 2 (for the common skeleton building see Refs. [58, 76, 93]).

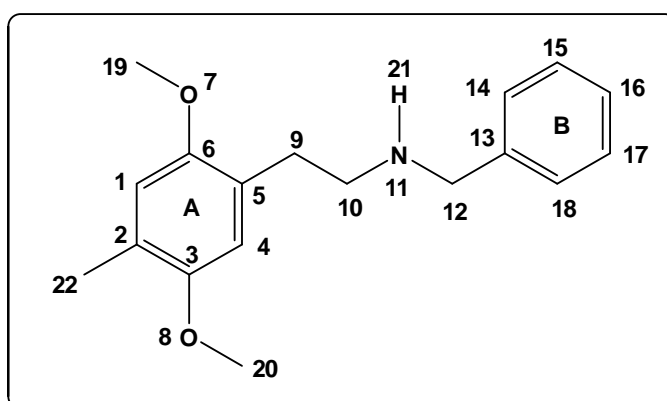


Figure 2. Numbering of the common skeleton

Besides rings A and B and the heavy atoms of the linker joining them, we have included in the common skeleton one of the N protons, the oxygen and carbon atoms of both MeO substituents of ring A and the first atom attached to position 2 in Fig. 2.

Calculations

All calculations were performed for the protonated forms. The electronic structure of all molecules was obtained with the Density Functional Theory (DFT) framework at the B3LYP/6-31g(d,p) level with full geometry optimization. The Gaussian suite of programs was used [102]. The values of the LARIs were obtained with the D-CENT-QSAR software [103]. Mulliken Population Analysis results were corrected to avoid negative electron populations [104]. Because it is not possible to solve the system of linear equations due to the lack of enough molecules, we employed linear multiple regression analysis (LMRA) to determine the local atomic properties involved in the variation of the biological activity through the series. The Statistica software was used for LMRA. We hypothesize that the variation of the numerical values of one or more local atomic reactivity indices of a number of atoms belonging to the common skeleton accounts for the variation of the biological activity. The role of the substituents is to modify the electronic structure of the common skeleton. We built a matrix containing the logarithm

of the dependent variable (the pK's) and the local atomic reactivity indices of the atoms of the common skeleton as independent variables. Molecule 41 was not included in the set due to convergence problems during the geometry optimization procedure. For the docking study, a crystal structure of a chimera protein of human 5-HT_{2B} and *E. coli* soluble cytochrome b562 was downloaded from the Protein Data Bank (4IB4, [53]) and prepared for use with the Autodock Vina software [105]. The site of ergotamine binding in 4IB4 was employed for the docking study. A 28x40x40 box was employed. A 4 Å volume around ergotamine was selected and all the receptor's residues inside it were allowed to change their conformation. The molecules in their fully optimized geometry were employed as the starting conformation (the geometry of molecule 41 was optimized at the MM/OPLS level). The lowest energy conformer produce by Autodock Vina was employed for further scrutiny. The docking results were analyzed with Autodock Vina and Discovery Studio Visualizer [106].

RESULTS

Local Molecular Orbital Structure

Tables 2 and 3 show the local MO structure of several important atoms.

Table 2. Local Molecular Orbital Structure of atoms 7, 8, 15 and 15

Mol	Atom 7 (O)	Atom 8 (O)	Atom 14 (C)	Atom 15 (C)
1 (98)	94π97π98π-103π104π113σ	95π97π98π-103π104σ123σ	93π94π96π-99π100π101π	87σ88σ96π-99π100π102π
2 (94)	90π93π94π- 99π109σ117σ	92σ93π94π- 99π100σ110σ	89π90π91π- 95π96π102σ	83σ84σ91π-95π96π98σ
3 (94)	90π93π94π-99π108σ110σ	92π93π94π-99π100σ115σ	89π90π91π- 95π96π103σ	89π90π91π- 95π96π98σ
4 (101)	96π100π101π-106π119σ128σ	98σ100π101π-106π107σ120	91π97π99π-102π103π110σ	91π97π99π-102π103π105σ
5 (89)	85π88π89π-94π96σ104σ	85σ88π89π-94π96σ105σ	79σ86π87π-90π91π92π	79σ80σ87π-90π91π93σ
6 (85)	82σ84π85π- 90π100σ104σ	82σ84π85π-90π92σ93σ	81π82π83π-86π87π92σ	74σ75σ83π-86π87π89σ
7 (85)	82σ84π85π- 90π92σ101σ	82π84π85π- 90π92σ106σ	80π81π83π-86π87π94σ	74σ80π83π-86π87π89σ
8 (92)	88π90π92π- 97π110σ111σ	87π88σ92π-97π99σ111σ	83π89π91π-93π94π101σ	83π89π91π-93π94π96σ
9 (85)	81π84π85π-90π100σ110σ	80σ81π85π- 90π109σ112σ	77σ82π83π-86π87π93σ	76σ77σ83π-86π87π89σ
10 (81)	78π80π81π- 86π96σ103σ	77π78π81π-86π102σ106σ	77π78π79π-82π83π88σ	71σ72σ79π-82π83π85σ
11 (81)	78π80π81π-86π96σ101σ	76σ78π81π- 86π103σ104σ	77π78π79π-82π83π89σ	71σ77π79π-82π83π84σ
12 (88)	84π86π88π- 93π106σ114σ	83σ84π88π- 93π114σ117σ	80π85π87π-89π90π96σ	80π85π87π-89π90π91σ
13 (85)	82π8485π-90π109σ110σ	81π82π85π-90π98σ109σ	81π82π83π-86π87π93σ	74σ76σ83π-86π87π89σ
14 (81)	78π80π81π- 86π95σ102σ	77π78π81π-86π102σ108σ	77π78π79π-82π83π88σ	70σ71σ79π-82π83π85σ
15 (81)	79π80π81π- 86π94σ102σ	78π79π81π-86π93σ103σ	77π78π79π-82π83π89σ	77π78π79π-82π83π84σ
16 (88)	85π87π88π-93π104σ114σ	84π85π88π-93π106σ114σ	80σ85π86π-89π90π96σ	84π85π86π-89π90π91σ
17 (89)	86π88π89π-94π103σ110σ	85π86π89π-94π114σ117σ	85π86π87π-90π91π97σ	78σ79σ87π-90π91π93σ
18 (85)	82π84π85π-91π92π98σ	81π82π85π-92π97σ103σ	74π82π83π-86π88π89π	74π82π83π-86π88π89π
19 (85)	83π84π85π-90π98σ105σ	82π83π85π-90π97σ108σ	81π82π83π-86π87π93σ	81π82π83π-86π87π88σ
20 (92)	89π91π92π-97π108σ116σ	88π89π92π-97π119σ122σ	88π89π90π-93π94π100σ	88π89π90π-93π94π95π
21 (93)	90π92π93π-98π107σ114σ	89π90π93π-98π118σ121σ	89π90π91π-94π95π101σ	79σ81π91π-94π95π97π
22 (89)	86π88π89π-94π103σ113σ	83σ86π89π-94π117σ121σ	75σ85π87π-90π91π96σ	74σ75σ87π-90π91π93σ
23 (89)	87π88π89π-94π102σ113σ	86π87π89π-94π101σ112σ	85π86π87π-90π91π97σ	75σ86π87π-90π91π92π
24 (96)	93π95π96π-101π112σ120σ	92π93π96π-101π123σ129σ	84π92π94π-97π98π104σ	84π92π94π-97π98π99π
25 (93)	89π92π93π-98π109σ116σ	89π92π93π-98π119σ123σ	88π89π90π-94π95π101σ	83σ90π91π-94π95π97σ
26 (89)	85π88π89π-94π98σ105σ	85π88π89π-94π98σ112σ	84π85π86π-90π91π96σ	77σ78σ86π-90π91π93σ
27 (89)	85π88π89π-94π108σ114σ	85π88π89π-94π113σ116σ	84π85π86π-90π91π97σ	84π85π86π-90π91π93σ
28 (96)	93π95π96π-101π116σ124σ	91π95π96π-101π124σ126σ	86π92π94π-97π98π104σ	86π92π94π-97π98π100π
29 (97)	93π96π97π-102π113σ120σ	93σ96π97π-102π123σ129σ	92π93π94π-98π99π106σ	84σ85σ94π-98π99π101π
30 (93)	89σ92π93π-98π102σ109σ	89σ92π93π-98π110σ116σ	88π89π90π-94π95π100σ	78σ79σ90π-94π95π97σ
31 (93)	91π92π93π-98π107σ110σ	90σ92π93π-98π115σ117σ	88π89π90π-94π95π101σ	79σ89π90π-94π95π97σ
32 (100)	97π99π100π-105π120σ129σ	96π99π100π-105π128σ129σ	95π96π98π-101π102π108σ	95π96π98π-101π102π104π
33 (101)	99π100π101π-106π117σ124σ	97σ100π101π-106π128σ131σ	96π97π98π-102π103π109σ	86σ88σ98π-102π103π105σ
34 (97)	95π96π97π-102π106σ113σ	93σ96π97π-102π106σ114σ	92π93π94π-98π99π104σ	81σ82σ94π-98π99π101σ
35 (97)	95π96π97π-102π116σ121σ	94π96π97π-102π110σ122σ	92π93π94π-98π99π105σ	91π93π94π-98π99π101σ
36 (104)	101π103π104π-109π122σ124σ	100π103π104π-109π113σ131σ	92π100π102π-105π106π107π	99π100π102π-105π106π107π
37 (97)	94π95π97π-101π102π112σ	95σ96π97π-101π102π110σ	93π95π96π-98π99π100π	89σ95π96π-98π99π100π
38 (93)	88σ89π93π-98π108σ112σ	88σ89π93π-98π105σ111σ	90π91π92π-94π95π96π	83σ91π92π-94π95π96π
39 (93)	89π90π93π-98π106σ108σ	89π90π93π- 98π105σ112σ	89π90π91π-94π95π101σ	79σ80σ91π-94π95π97σ
40 (100)	95σ96π100π-105π118σ120σ	95σ96π100π-105π118σ120σ	92π97π99π-101π102π108σ	92π97π99π-101π102π104π
42 (83)	79π82π83π- 88π105σ107σ	78σ79π83π-88π96σ105σ	72σ80π81π-84π85π86π	71σ72σ81π-84π86π87π
43 (83)	80π82π83π- 88π98σ105σ	79π80π83π-88π96σ105σ	79π80π81π-84π86π91σ	72σ80π81π-84π85π86π
44 (90)	86π88π90π- 95π105π108σ	85σ86π90π- 95π117σ123σ	80π87π89π-91π93π99σ	80π87π89π-91π93π94σ

Table 3. Local Molecular Orbital Structure of atoms 18, 19 and 20

Mol	Atom 18 (C)	Atom 19 (C)	Atom 20 (C)
1 (98)	88σ94π96π-99π100π102σ	91σ92σ93σ-107σ108σ109σ	90σ91σ92σ-104σ114σ117σ
2 (94)	82σ83σ91π-95π96π98σ	87σ88σ90σ-102σ103σ104σ	86σ87σ88σ-100σ110σ112σ
3 (94)	82σ83σ91π-95π96π98σ	87σ88σ90σ-103σ105σ106σ	86σ87σ88σ-100σ108σ109σ
4 (101)	89σ97π99π-102π103π105σ	94σ95σ96σ-114σ115σ116σ	93σ94σ95σ-107σ117σ121σ
5 (89)	79σ86π87π-90π91π93σ	80σ81σ84σ-95σ98σ99σ	82σ83σ84σ-96σ105σ108σ
6 (85)	74σ75σ83π-86π87π89σ	77σ78σ80σ-95σ96σ97σ	78σ79σ80σ-92σ93σ100σ
7 (85)	72σ74σ83π-86π87π89σ	76σ77σ81σ-92σ94σ96σ	78σ79σ81σ-92σ99σ100σ
8 (92)	80σ89π91π-93π94π96σ	84σ85σ87σ-106σ107σ109σ	85σ86σ87σ-99σ108σ112σ
9 (85)	77σ82π83π-86π87π89σ	78σ79σ81σ-93σ95σ96σ	79σ80σ81σ-94σ95σ97σ
10 (81)	70σ71σ79π-82π83π85σ	74σ75σ77σ-88σ90σ93σ	75σ76σ77σ-90σ91σ93σ
11 (81)	69σ71σ79π-82π83π84σ	74σ75σ78σ-89σ91σ92σ	75σ76σ78σ-91σ92σ93σ
12 (88)	77σ85π87π-89π90π91σ	82σ83σ84σ-99σ100σ101σ	82σ83σ84σ-101σ102σ103σ
13 (85)	74σ76σ83π-86π87π88σ	80σ81σ82σ-93σ94σ95σ	80σ81σ82σ-95σ100σ101σ
14 (81)	69σ70σ79π-82π83π84σ	75σ76σ78σ-88σ89σ90σ	75σ76σ78σ-91σ96σ98σ
15 (81)	70σ78π79π-82π83π84σ	75σ76σ78σ-89σ91σ92σ	75σ76σ78σ-91σ96σ97σ
16 (88)	76σ85π86π-89π90π91σ	82σ83σ84σ-101σ102σ103σ	82σ83σ84σ-103σ106σ107σ
17 (89)	78σ79σ87π-90π91π93σ	84σ85σ86σ-97σ98σ99σ	84σ85σ86σ-99σ104σ105σ
18 (85)	70σ73σ83π-86π88π89π	77σ78σ81σ-94σ95σ97σ	79σ80σ81σ-101σ102σ107σ
19 (85)	72σ82π83π-86π87π88σ	78σ80σ82σ-93σ95σ96σ	78σ80σ82σ-95σ98σ99σ
20 (92)	88π89π90π-93π94π95σ	87σ88σ89σ-105σ106σ107σ	87σ88σ89σ-107σ109σ110σ
21 (93)	81σ89π91π-94π95π97σ	84σ87σ90σ-101σ102σ103σ	86σ87σ90σ-103σ108σ109σ
22 (89)	74σ75σ87π-90π91π92σ	80σ83σ86σ-96σ97σ98σ	82σ83σ86σ-104σ106σ107σ
23 (89)	75σ86π87π-90π91π92σ	83σ86σ87σ-97σ99σ100σ	83σ86σ87σ-99σ102σ103σ
24 (96)	81σ92π94π-97π98π99σ	89σ90σ93σ-109σ110σ111σ	89σ90σ93σ-111σ113σ114σ
25 (93)	83σ89π90π-94π95π97σ	85σ87σ88σ-101σ102σ103σ	86σ87σ88σ-101σ102σ109σ
26 (89)	76σ77σ86π-90π91π93σ	82σ83σ85σ-96σ99σ102σ	82σ83σ85σ-98σ99σ105σ
27 (89)	77σ85π86π-90π91π93σ	81σ83σ85σ-97σ100σ101σ	82σ83σ85σ-98σ99σ104σ
28 (96)	82σ92π94π-97π98π100σ	89σ90σ91σ-107σ110σ111σ	89σ90σ91σ-106σ108σ112σ
29 (97)	83σ84σ94π-98π99π101π	90σ91σ93σ-105σ106σ107σ	90σ91σ93σ-105σ106σ113σ
30 (93)	78σ79σ90π-94π95π97σ	86σ87σ89σ-100σ103σ104σ	86σ87σ89σ-102σ109σ111σ
31 (93)	79σ89π90π-94π95π97σ	86σ88σ89σ-101σ104σ105σ	87σ88σ89σ-102σ103σ108σ
32 (100)	95π96π98π-101π102π104σ	94σ95σ96σ-114σ115σ116σ	93σ94σ95σ-110σ116σ118σ
33 (101)	86σ88σ98π-102π103π105σ	92σ95σ97σ-109σ110σ111σ	94σ95σ97σ-109σ110σ117σ
34 (97)	80σ82σ94π-98π99π101σ	88σ91σ93σ-104σ105σ107σ	90σ91σ93σ-106σ107σ113σ
35 (97)	81σ93π94π-98π99π101σ	87σ92σ93σ-105σ108σ109σ	90σ92σ93σ-106σ112σ113σ
36 (104)	88σ100π102π-105π106π107σ	95σ98σ99σ-112σ114σ116σ	97σ98σ99σ-113σ121σ123σ
37 (97)	93π95π96π-98π99π100π	90σ91σ92σ-105σ107σ108σ	94σ95σ97σ-101σ102σ111σ
38 (93)	83σ91π92π-94π95π96π	87σ88σ89σ-100σ102σ105σ	87σ88σ89σ-102σ107σ108σ
39 (93)	78σ80σ91π-94π95π97σ	88σ89σ90σ-101σ102σ103σ	88σ89σ90σ-103σ107σ108σ
40 (100)	86σ97π99π-101π102π104σ	94σ95σ96σ-111σ112σ113σ	94σ95σ96σ-115σ116σ117σ
42 (83)	71σ72σ81π-84π85π86π	73σ74σ79σ-90σ91σ92σ	76σ77σ79σ-92σ100σ101σ
43 (83)	71σ72σ81π-84π85π86π	73σ74σ79σ-91σ94σ95σ	76σ77σ79σ-91σ92σ100σ
44 (90)	78σ87π89π-91π93π94σ	81σ84σ86σ-101σ103σ104σ	83σ84σ86σ-98σ100σ107σ

Linear Multiple Regression Results

Results for the 5-HT_{2B} receptor binding affinity of the whole set of molecules (I)

$$pK_i = 18.70 - 5126\omega_{12} - 1.87Q_3 - 0.74s_6 + 1.35S_{19}^E(HOMO - 2)^* + 18.22F_7(LUMO + 2)^* - 2.66F_{20}(LUMO + 1)^* + 0.27S_{15}^E(HOMO)^* + 1.64Q_9^{\max} \quad (2)$$

with $n=43$, $R=0.95$, $R^2=0.91$, $\text{adj-}R^2=0.89$, $F(8,34)=41.87$ ($p<0.000001$) and a standard error of estimate of 0.21. No outliers were detected and no residuals fall outside the $\pm 2.00 \sigma$ limits. Here, ω_{12} is the local atomic electrophilicity of atom 12 (a carbon atom linking NH and ring B), Q_3 is the net charge of atom 3 (in ring A), s_6 is the local atomic softness of atom 6 (in ring A), $S_{19}^E(HOMO - 2)^*$ is the orbital electrophilic superdelocalizability of the third highest occupied MO localized on atom 19 (a carbon atom of OMe), $F_7(LUMO + 2)^*$ is the Fukui index of the third lowest vacant MO localized on atom 7 (an oxygen atom of OMe), $F_{20}(LUMO + 1)^*$ is the Fukui index of the second lowest vacant MO localized on atom 20 (a carbon atom of OMe), $S_{15}^E(HOMO)^*$ is the orbital electrophilic superdelocalizability of the highest occupied MO localized on atom 15 (in ring B) and Q_9^{\max} is

the maximal amount of charge atom 9 may receive (one of the carbon atoms of the NH-ring A linker). Tables 4 and 5 show, respectively, the beta coefficients, the results of the t-test for significance of coefficients and the matrix of squared correlation coefficients for the variables appearing in Eq. 2. Figure 3 shows the plot of observed *vs.* calculated values.

Table 4. Beta coefficients and t-test for significance of coefficients in Eq. 2

	Beta	t(34)	p-level
ω_{12}	-0.55	-9.30	<0.000001
Q_3	-0.47	-7.61	<0.000001
s_6	-0.36	-5.89	<0.000001
$S_{19}^E(HOMO-2)^*$	0.41	6.95	<0.000001
$F_7(LUMO+2)^*$	0.28	5.18	<0.000001
$F_{20}(LUMO+1)^*$	-0.25	-4.07	<0.0003
$S_{15}^E(HOMO)^*$	0.21	3.65	<0.0009
Q_9^{\max}	0.16	2.64	<0.01

Table 5. Matrix of squared correlation coefficients for the variables in Eq. 2

	ω_{12}	Q_3	s_6	$S_{19}^E(HOMO-2)^*$	$F_7(LUMO+2)^*$	$F_{20}(LUMO+1)^*$	$S_{15}^E(HOMO)^*$
Q_3	0.003	1.00					
s_6	0.02	0.14	1.00				
$S_{19}^E(HOMO-2)^*$	0.07	0.09	0.004	1.00			
$F_7(LUMO+2)^*$	0.008	0.04	0.04	0.01	1.00		
$F_{20}(LUMO+1)^*$	0.15	0.02	0.005	0.02	0.004	1.00	
$S_{15}^E(HOMO)^*$	0.0009	0.01	0.002	0.02	0.004	0.04	1.00
Q_9^{\max}	0.005	0.03	0.07	0.01	0.03	0.07	0.06

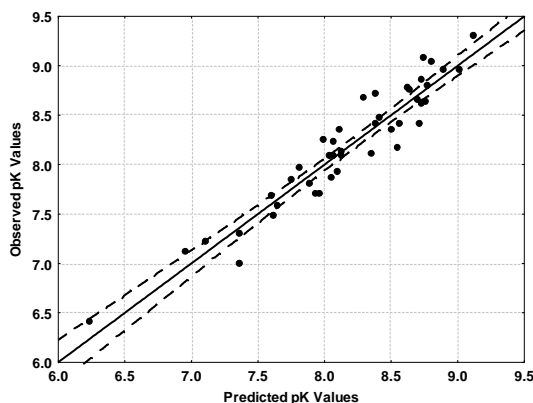


Figure 3. Plot of predicted *vs.* observed pK values (Eq. 2). Dashed lines denote the 95% confidence interval

Table 5 shows that there are no significant internal correlations between independent variables. The associated statistical parameters of Eq. 2 (Table 4) show that this equation is statistically significant and that the variation of a group of eight local atomic reactivity indices belonging to the common skeleton explains about 89% of the variation of the 5-HT_{2B} receptor binding affinity. Figure 3, spanning about three orders of magnitude, shows that there is a good correlation of observed *versus* calculated values and that almost all points are inside the 95% confidence interval.

Results for 5-HT_{2B} receptor binding affinity of set II

$$pK_i = 8.46 - 0.97S_{15}^E(HOMO-2)^* - 6.24F_{20}(HOMO-1)^* - 0.35S_8^E(HOMO-2)^* + 0.51S_{18}^E(HOMO)^* \quad (3)$$

with $n=16$, $R=0.94$, $R^2=0.88$, adjusted $R^2=0.83$, $F(4,11)=19.64$ ($p<0.00006$) and a standard error of estimate of 0.19. No outliers were detected and no residuals fall outside the $\pm 2.00\sigma$ limits. Here, $S_{15}^E(HOMO-2)^*$ is the orbital electrophilic superdelocalizability of the third highest occupied MO localized on atom 15 (in ring B), $F_{20}(HOMO-1)^*$ is the Fukui index of the second highest MO localized on atom 20 (the carbon atom of a OMe substituent), $S_8^E(HOMO-2)^*$ is the orbital electrophilic superdelocalizability of the third highest occupied MO localized on atom 8 (the oxygen atom of a MeO substituent) and $S_{18}^E(HOMO)^*$ is the orbital electrophilic superdelocalizability of the highest occupied MO localized on atom 18 (in ring B). Tables 6 and 7 show, respectively, the beta coefficients, the results of the t-test for significance of coefficients and the matrix of squared correlation coefficients for the variables appearing in Eq. 3. Figure 4 shows the plot of observed vs. calculated values.

Table 6. Beta coefficients and t-test for significance of coefficients in Eq. 3

	Beta	t(11)	p-level
$S_{15}^E(HOMO-2)^*$	-0.66	-5.77	<0.0001
$F_{20}(HOMO-1)^*$	-0.69	-5.78	<0.0001
$S_8^E(HOMO-2)^*$	-0.44	-3.64	<0.004
$S_{18}^E(HOMO)^*$	0.30	2.65	<0.02

Table 7. Matrix of squared correlation coefficients for the variables in Eq. 3

	$S_{15}^E(HOMO-2)^*$	$F_{20}(HOMO-1)^*$	$S_8^E(HOMO-2)^*$
$F_{20}(HOMO-1)^*$	0.03	1.00	
$S_8^E(HOMO-2)^*$	0.006	0.17	1.00
$S_{18}^E(HOMO)^*$	0.09	0.008	0.03

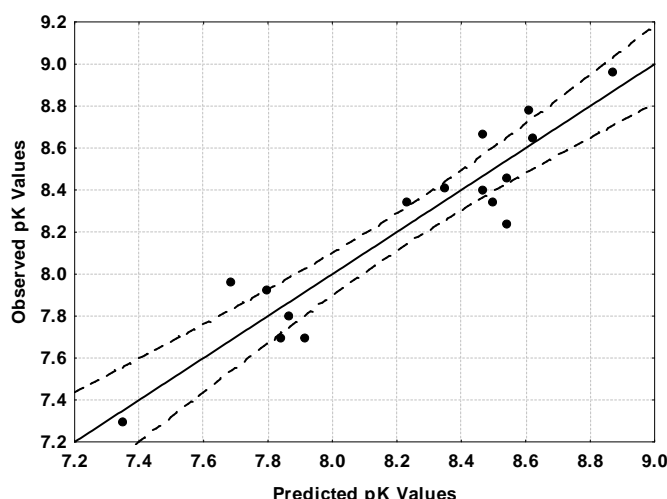


Figure 4. Plot of predicted vs. observed pK values (Eq. 3). Dashed lines denote the 95% confidence interval

Table 7 shows that there are no significant internal correlations between independent variables. The associated statistical parameters of Eq. 3 (Table 6) show that this equation is statistically significant and that the variation of a group of four local atomic reactivity indices belonging to the common skeleton explains about 83% of the variation

of the 5-HT_{2B} receptor binding affinity. Figure 4, spanning about 1.7 orders of magnitude, shows that there is a good correlation of observed *versus* calculated values and that almost all points are inside the 95% confidence interval.

Results for 5-HT_{2B} receptor binding affinity of set III

$$pK_i = 37.71 + 313.93Q_{19} + 14.50Q_4 - 6.90Q_{21}^{\max} + 0.17S_7^N(LUMO + 2)^* - 0.31S_{14}^E(HOMO - 1)^* + 3.03F_{19}(LUMO + 1)^* - 0.46S_8^N(LUMO + 2)^* \quad (4)$$

with $n=27$, $R=0.99$, $R^2=0.97$, adjusted $R^2=0.96$, $F(7,19)=97.08$ ($p<0.000001$) and a standard error of estimate of 0.14. No outliers were detected and no residuals fall outside the $\pm 2.00\sigma$ limits. Here, Q_{19} is the net charge of atom 19 (the carbon atom of a MeO substituent), Q_4 is the net charge of atom 4 (in ring A), Q_{21}^{\max} is the maximal amount of charge atom 21 (the proton of the NH group) may receive, $S_7^N(LUMO + 2)^*$ is the orbital nucleophilic superdelocalizability of the third lowest vacant MO localized on atom 7 (the oxygen atom of a MeO substituent), $S_{14}^E(HOMO - 1)^*$ is the orbital electrophilic superdelocalizability of the second highest MO localized on atom 14 (in ring B), $F_{19}(LUMO + 1)^*$ is the Fukui index of the second lowest vacant MO localized on atom 19 (the carbon atom of a MeO substituent) and $S_8^N(LUMO + 2)^*$ is the orbital nucleophilic superdelocalizability of the third lowest vacant MO localized on atom 8 (a carbon atom of the NH-ring A linker). Tables 8 and 9 show, respectively, the beta coefficients, the results of the t-test for significance of coefficients and the matrix of squared correlation coefficients for the variables appearing in Eq. 4. Figure 5 shows the plot of observed *vs.* calculated values.

Table 8. Beta coefficients and t-test for significance of coefficients in Eq. 4

	Beta	t(19)	p-level
Q_{19}	0.89	18.83	<0.000001
Q_4	0.53	12.27	<0.000001
Q_{21}^{\max}	-0.24	-4.99	<0.00008
$S_7^N(LUMO + 2)^*$	0.17	4.08	<0.0006
$S_{14}^E(HOMO - 1)^*$	-0.18	-4.10	<0.0006
$F_{19}(LUMO + 1)^*$	0.17	4.04	<0.0007
$S_8^N(LUMO + 2)^*$	-0.14	-3.18	<0.005

Table 9. Matrix of squared correlation coefficients for the variables in Eq. 4

	Q_{19}	Q_4	Q_{21}^{\max}	$S_7^N(LUMO + 2)^*$	$S_{14}^E(HOMO - 1)^*$	$F_{19}(LUMO + 1)^*$
Q_4	0.08	1.00				
Q_{21}^{\max}	0.22	0.12	1.00			
$S_7^N(LUMO + 2)^*$	0.01	0.06	0.001	1.00		
$S_{14}^E(HOMO - 1)^*$	0.02	0.02	0.04	0.08	1.00	
$F_{19}(LUMO + 1)^*$	0.0009	0.005	0.05	0.005	0.05	1.00
$S_8^N(LUMO + 2)^*$	0.06	0.006	0.0004	0.02	0.005	0.13

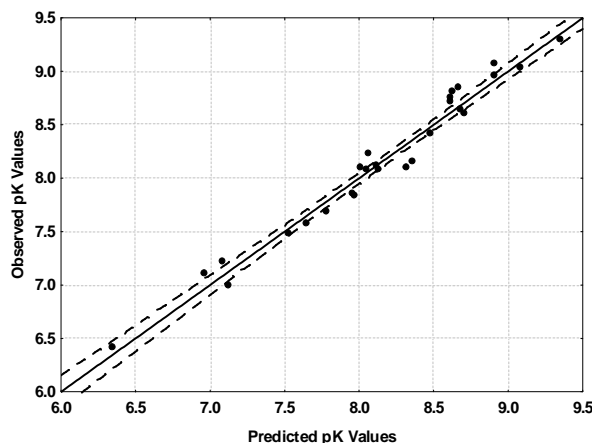


Figure 5. Plot of predicted *vs.* observed pK values (Eq. 4). Dashed lines denote the 95% confidence interval

Table 9 shows that there are no significant internal correlations between independent variables. The associated statistical parameters of Eq. 4 (Table 8) show that this equation is statistically significant and that the variation of a group of seven local atomic reactivity indices belonging to the common skeleton explains about 96% of the variation of the 5-HT_{2B} receptor binding affinity. Figure 5, spanning about three orders of magnitude, shows that there is a good correlation of observed *versus* calculated values and that almost all points are inside the 95% confidence interval.

DOCKING RESULTS

Figs. 6 to 16 show the docking results. Tables 10 and 11 show, respectively, the definitions of the colors representing the interactions and the list, type and distance of the interactions (see also Fig. 2).

Table 10. List of colors for docking figures analysis

Interaction	Color name	RGB
Pi-alkyl (hydrophobic)	Cotton candy	(255,200,255)
Alkyl (hydrophobic)	Cotton candy	(255,200,255)
Pi-sigma (hydrophobic)	Heliotrope	(200,100,255)
Carbon-hydrogen bond	Honeydew	(220,255,220)
Conventional H-bond	Lime	(0,255,0)
Salt bridge (attractive charge)	Orange peel	(255,150,0)
Pi-anion	Orange peel	(255,150,0)
Pi-Pi stacked	Neon pink	(255,100,200)
Pi-Pi T shaped	Neon pink	(255,100,200)
Halogen	Aqua	(0,255,255)
Attractive charge	Orange peel	(255,150,0)
Carbon-hydrogen bond, halogen	Honeydew	(220,255,220)
Pi-sulphur	Tangerine yellow	(255,200,0)
Unfavorable donor-donor	Red	(255,10,0)
Unfavorable positive-positive	Red	(255,10,0)
Pi-cation	Orange peel	(255,150,0)
Unfavorable acceptor-acceptor	Red	(255,10,0)

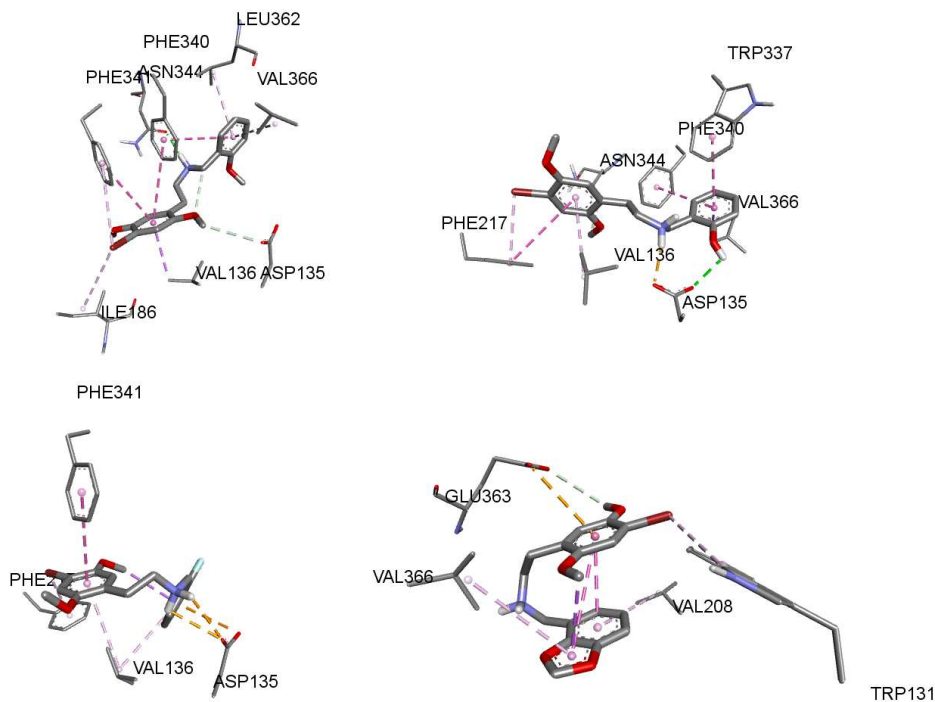


Figure 6. Docking results for molecules 1 (upper left), 2 (upper right), 3 (lower left) and 4 (lower right)

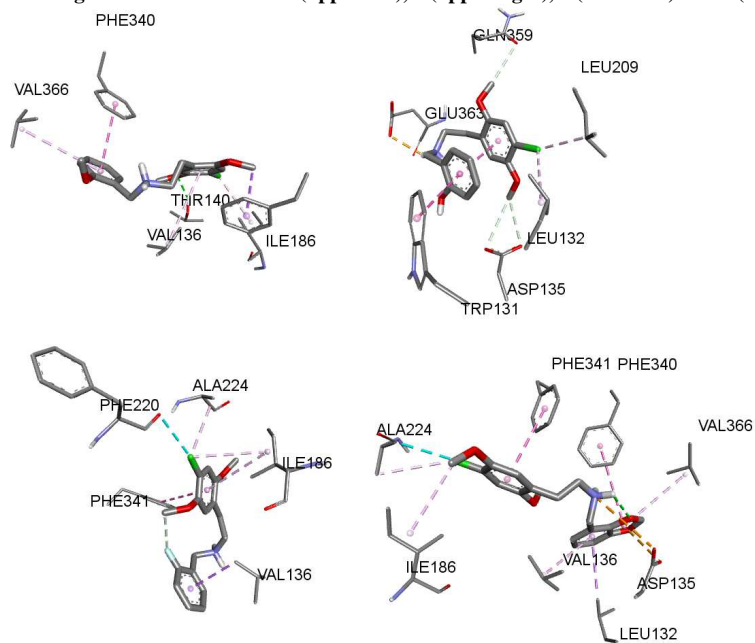


Figure 7. Docking results for molecules 5 (upper left), 6 (upper right), 7 (lower left) and 8 (lower right)

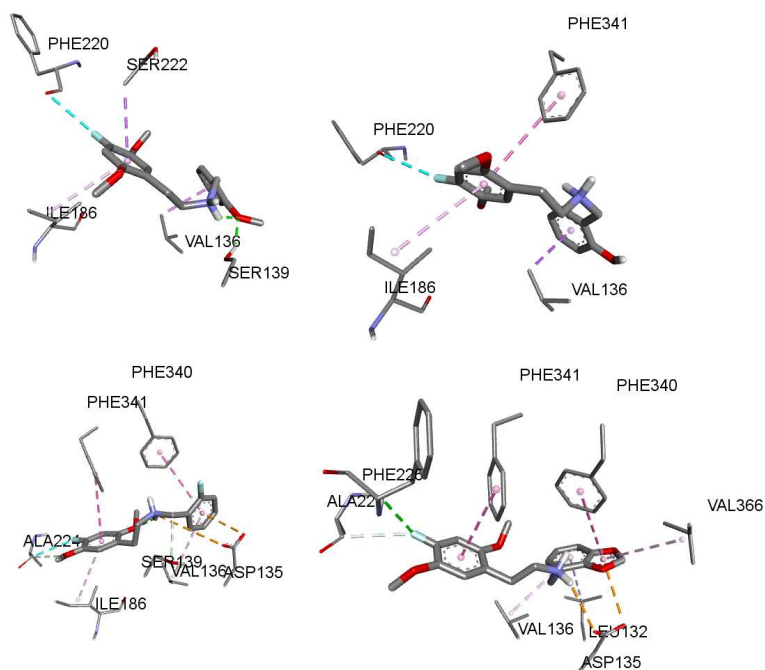


Figure 8. Docking results for molecules 9 (upper left), 10 (upper right), 11 (lower left) and 12 (lower right)

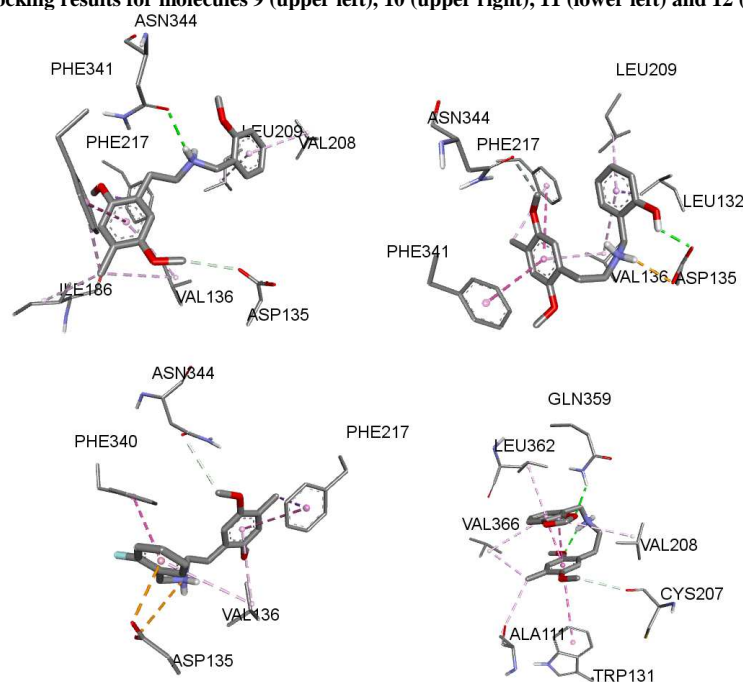


Figure 9. Docking results for molecules 13 (upper left), 14 (upper right), 14 (lower left) and 16 (lower right)

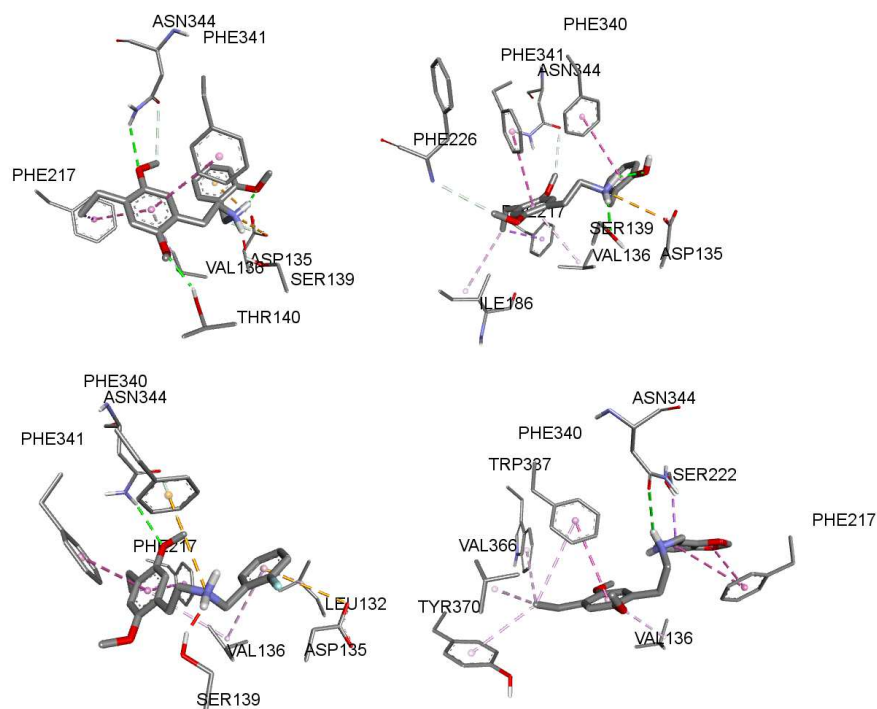


Figure 10. Docking results for molecules 17 (upper left), 18 (upper right), 19 (lower left) and 20 (lower right)

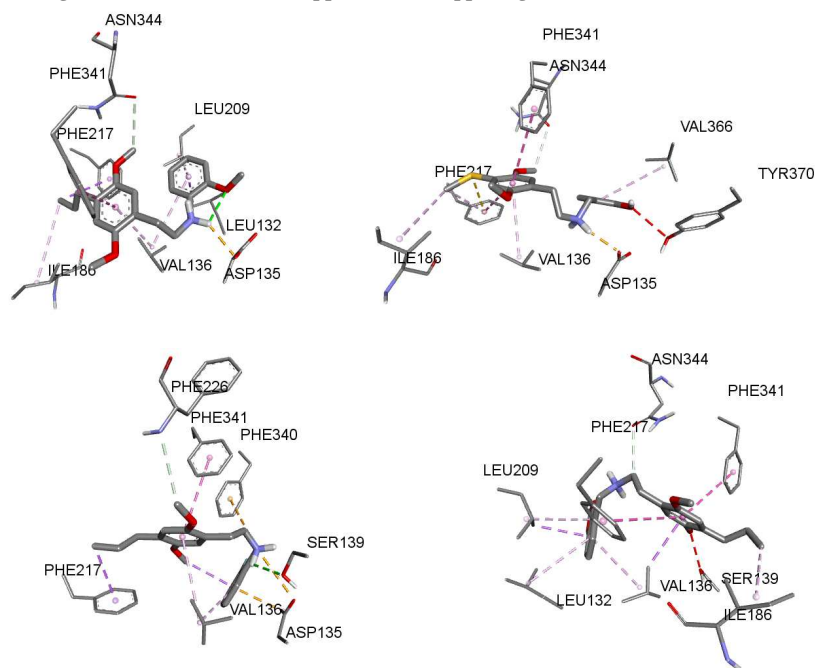


Figure 11. Docking results for molecules 21 (upper left), 22 (upper right), 23 (lower left) and 24 (lower right)

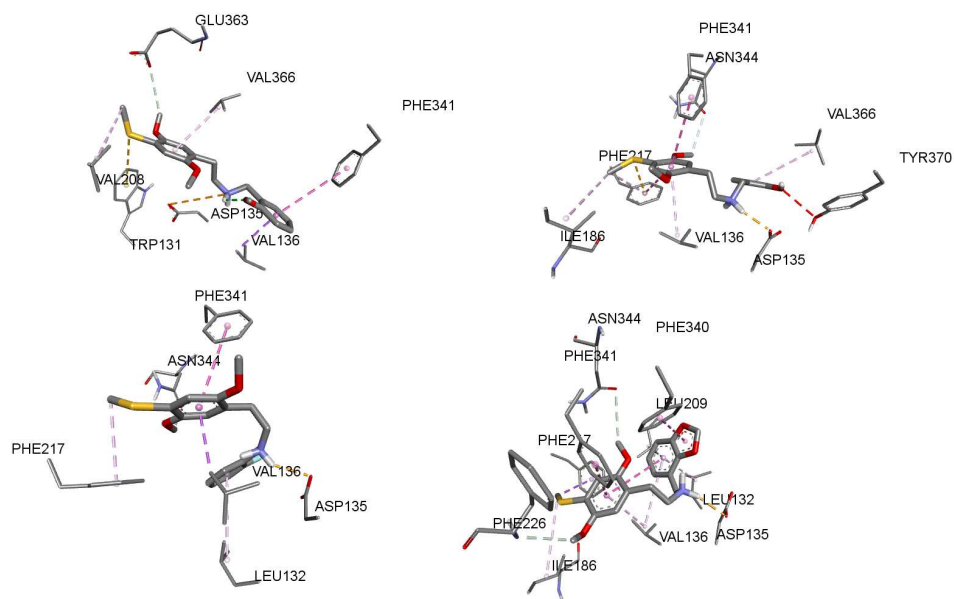


Figure 12. Docking results for molecules 25 (upper left), 26 (upper right), 27 (lower left) and 28 (lower right)

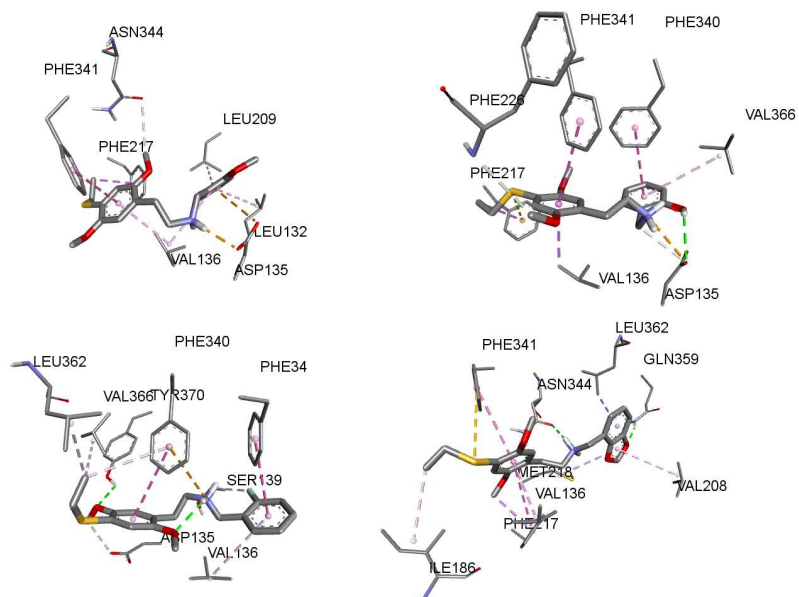


Figure 13. Docking results for molecules 29 (upper left), 30 (upper right), 31 (lower left) and 32 (lower right)

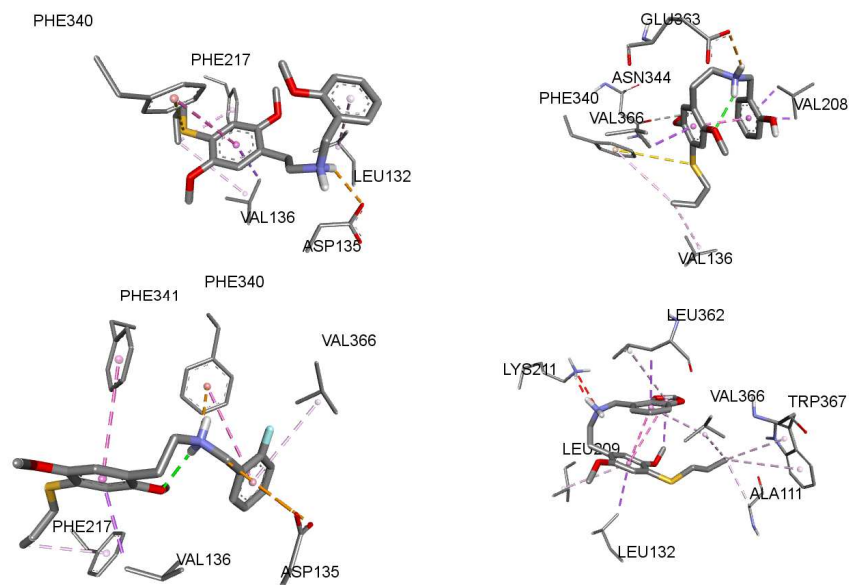


Figure 14. Docking results for molecules 33 (upper left), 34 (upper right), 35 (lower left) and 36 (lower right)

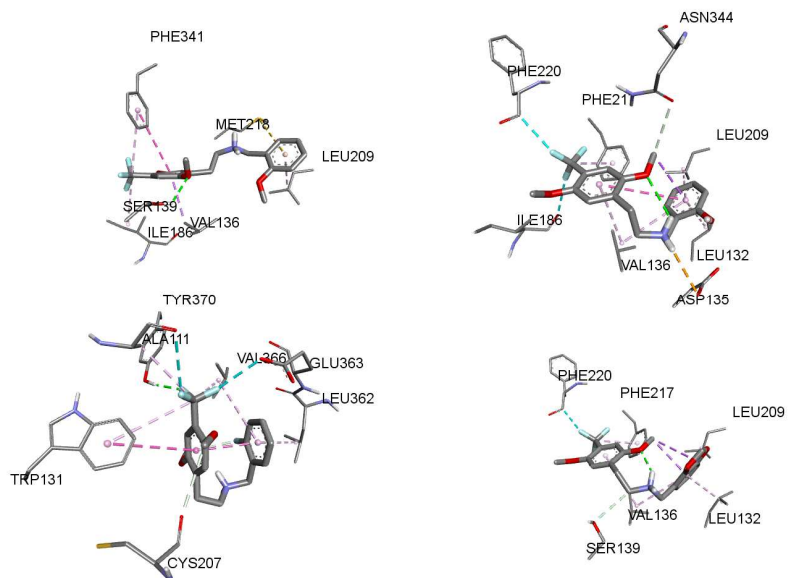


Figure 15. Docking results for molecules 37 (upper left), 38 (upper right), 39 (lower left) and 40 (lower right)

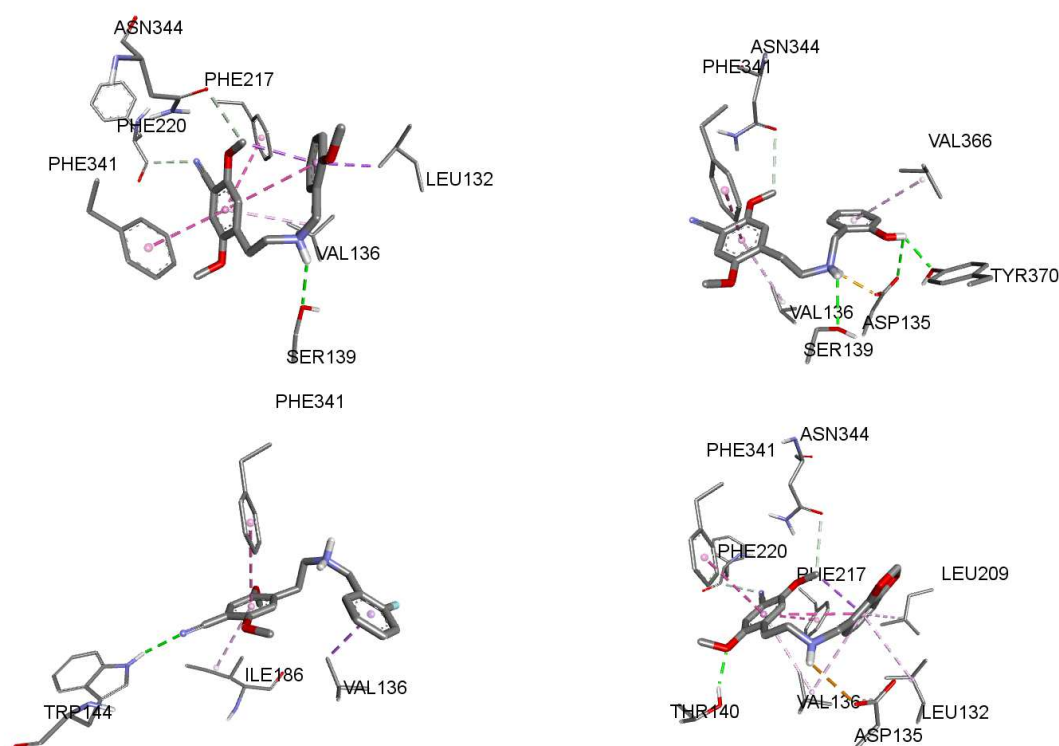


Figure 16. Docking results for molecules 41 (upper left), 42 (upper right), 43 (lower left) and 44 (lower right)

TABLE 11. Summary of inter- and intramolecular interactions of N-Benzylphenethylamines with the 5-HT_{2B} receptor site from Figs. 6-16

Mol.	Interactions
1+	π - π T shaped of ring A with Phe-340 (5.44Å) and Phe-341(5.34Å), π - σ of ring A with Val-136 (3.87Å), carbon H-bond between C of 2-OMe from ring A with Asp-135 (3.63Å), π -alkyl of Br with Phe-341 (5.01Å), alkyl interaction of Br with Ile-186 (5.39Å), π - π T shaped of ring B with Phe-340 (5.64Å), π -alkyl of ring B with Val-366 (5.40Å) and Leu-362 (4.43Å), conventional H-bond between H21 and Asn-344 (2.01Å). <i>Intramolecular carbon H-bond between O7 and C12 (3.75Å).</i>
2	π - π stacking of ring A with Phe-217 (5.26Å), π -alkyl of Br with Phe-217 (4.06Å), π -alkyl of ring A with Val-136 (4.99Å), carbon H-bond between C19 and Asn-344 (3.80Å), π - π T shaped of ring B with Phe-340 (4.75Å), π - π stacking of ring B with Trp-337 (4.19Å), π - σ of ring B with Val-366 (3.78Å), conventional H-Bond between H of 2-OH in ring B and Asp-135 (2.40Å), salt bridge between H21 and Asp-135 (2.12Å).
3#	π - π T shaped of ring A with Phe-341 (4.99Å), π -alkyl of ring A with Val-136 (4.87Å), π -alkyl of Br with Phe-217 (4.13Å), π -alkyl of ring B with Val-136 (4.85Å), π -anion with ring B and Asp-135 (3.88Å), salt bridge between the two hydrogen atoms of N11 and Asp-135 (2.80Å and 3.00Å). <i>Intramolecular π-σ interaction of C20 and ring B (3.63Å).</i>
4*#	π -anion of ring A with Glu-363 (4.01Å), π -alkyl of Br with Trp-131 (4.90Å), carbon H-bond between C20 and Glu-363 (3.61Å), π -alkyl of ring B with Val-208 (5.49Å), π -alkyl of methylenedioxy moiety with Val-366 (5.10Å). <i>Intramolecular π-π stacking between ring A and ring B (3.96Å), intramolecular π-π stacking between ring A and methylenedioxy moiety (5.18Å), intramolecular π-σ interaction between C19 and methylenedioxy moiety (3.77Å).</i>
5	π -alkyl of ring A with Val-136 (5.17Å), π - σ of C19 with Phe-217 (3.55Å), alkyl interaction of Cl with Ile-186 (4.06Å), conventional H-bond between O8 and Thr-140 (2.35Å), π - π stacking of ring B and Phe-340 (4.17Å), π -alkyl of ring B and Val-366 (5.09Å).
6*	Carbon H-bond between C19 and Gln-359 (3.61Å), carbon H-bond between C20 and the two oxygen atoms of Asp-135 (3.48Å and 3.68Å), alkyl interaction of Cl with Leu-132 (4.47Å) and Leu-209 (3.79Å), π - π stacking of ring B with Trp-131 (4.38Å), salt bridge between H21 and Glu-363 (2.53Å). <i>Intramolecular π-π stacking between ring A and ring B (3.74Å).</i>
7+	π - π T shaped of ring A with Phe-341 (5.36Å), π -alkyl of ring A with Ile-186 (4.82Å), alkyl interaction of Cl with Ile-186 (4.40Å) and Ala-224 (3.61Å), halogen interaction of Cl with Phe-220 (3.23Å), π - σ of ring B and Val-136 (3.48Å). <i>Intramolecular carbon H-bond between F and C20 (3.23Å).</i>
8+	π - π T shaped of ring A with Phe-341 (4.76Å), alkyl interaction of Cl with Ile-186 (4.78Å) and Ala-224 (4.20Å), halogen interaction of Cl with Ala-224 (3.23Å), π - σ of ring B and Leu-132 (3.89Å), π -alkyl of ring B and Val-136 (4.83Å), π -anion of methylenedioxy moiety and Asp-135 (3.71Å), π - π T shaped of methylenedioxy moiety and Phe-340 (5.26Å), π -alkyl of methylenedioxy moiety with Val-366 (4.96Å), attractive charge interaction between N11 and Asp-135 (4.43Å). <i>Intramolecular H-bond between H21 and O from methylenedioxy moiety (2.87Å).</i>
9+	π - σ of ring A with Ser-222 (3.99Å), π -alkyl of ring A with Ile-186 (4.78Å), halogen interaction of F with Phe-220 (3.36Å), π - σ of ring B with Val-136 (3.51Å), conventional H-bond between O from 2-OMe in ring B and Ser-139 (2.05Å). <i>Intramolecular H-bond between O from 2-OMe in ring B and H21 (2.04Å).</i>
10	π - π T shaped of ring A with Phe-341 (5.43Å), π -alkyl of ring A with Ile-186 (4.80Å), halogen interaction of F with Phe-220 (3.45Å), π - σ of ring B with Val-136 (3.58Å).
11+	π - π T shaped of ring A with Phe-341 (4.95Å), π -alkyl of ring A with Ile-186 (5.26Å), halogen interaction of F with Ala-224 (3.30Å), carbon H-bond of O8 with Ala-224 (3.57Å), π - π stacking of ring B with Phe-340 (5.25Å), π -anion of ring B with Asp-135 (3.49Å), π -alkyl of ring B with Val-136 (5.34Å), attractive charge interaction between N11 and Asp-135 (5.27Å), carbon H-bond between C12 and Ser-139 (3.48Å). <i>Intramolecular H-bond between H21 and O7 (2.42Å).</i>

12	π - π T shaped of ring A with Phe-341 (4.75Å), conventional H-bond between F and Phe-226 (2.97Å), carbon H-bond of F with Ala-224 (3.39Å), π - π T shaped of methylenedioxy moiety and Phe-340 (5.48Å), π -anion of methylenedioxy moiety and Asp-135 (3.91Å), π -alkyl of ring B with Val-136 (4.89Å) and Leu-132 (4.93Å), attractive charge interaction between N11 and Asp-135 (3.12Å).
13	π - π T shaped of ring A with Phe-341 (4.94Å), π -alkyl of ring A with Val-136 (5.18Å), alkyl interaction of C from 4-Me with Val-136 (5.32Å) and Ile-186 (5.44Å), π -alkyl of C from 4-Me with Phe-341 (5.27Å), carbon H-bond of C20 with Asp-135 (3.49Å), π - σ of C19 with Phe-217 (3.90Å), π -alkyl of ring B with Val-208 (5.05Å) and Leu-209 (4.56Å), conventional H-bond between H21 and Asn-344 (2.36Å).
14	π - π T shaped of ring A with Phe-341 (5.07Å), π - π stacking of ring A with Phe-217 (5.99Å), π -alkyl of ring A with Val-136 (4.70Å), π -alkyl of C from 4-Me with Phe-217 (4.57Å), carbon H-bond between C20 and Asn-344 (3.62Å), π -alkyl of ring B with Val-136 (5.28Å) and Leu-209 (4.92Å), π - σ of ring B with Leu-132 (3.72Å), conventional H-bond between H of 2-OH in ring B and Asp-135 (2.21Å), salt bridge between H21 and Asp-135 (2.60Å).
15	π - π stacking of ring A with Phe-217 (5.28Å), π -alkyl of ring A with Val-136 (5.24Å), π - σ of C from 4-Me with Phe-217 (3.88Å), carbon H-bond between C20 and Asn-344 (3.74Å), π - π stacking of ring B with Phe-340 (5.29Å), π -alkyl of ring B with Val-136 (5.40Å), π -anion of ring B with Asp-135 (3.33Å), attractive charge interaction of N11 and Asp-135 (4.49Å).
16**+	π - π T shaped of ring A with Trp-131 (5.62Å), alkyl interaction of C from 4-Me with Ala-111 (4.46Å) and Val-366 (3.78Å), π -alkyl of ring B with Val-366 (4.90Å) and Leu-362 (4.39Å), π -alkyl of methylenedioxy moiety with Val-208 (5.23Å), conventional H-bond between O from methylenedioxy moiety and Gln-359 (2.28Å), <i>Intramolecular H-bond between H21 and O7 (2.23Å), intramolecular π-π stacking of ring A with ring B (3.75Å) and methylenedioxy moiety (3.82Å).</i>
17+	π - π T shaped of ring A with Phe-341 (5.42Å), π -alkyl of ring A with Val-136 (5.31Å), π - π stacking of ring A with Phe-217 (5.30Å), conventional H-bond between O7 and Thr-140 (2.14Å), conventional H-bond between O8 and Asn-344 (2.61Å), π - σ of terminal C from 4-Et with Phe-217 (3.56Å), π -anion of ring B with Asp-135 (3.97Å), carbon H-bond between C12 and Asp-135 (3.58Å), attractive charge interaction of N11 with Asp-135 (4.27Å), unfavorable donor-donor interaction of H21 with Ser-139 (1.73Å). <i>Intramolecular H-bond between O from 2-OMe in ring B and H21 (2.15Å).</i>
18+	π - π T shaped of ring A with Phe-341 (5.08Å), π -alkyl of ring A with Val-136 (4.47Å), π - σ of terminal C from 4-Et with Phe-217 (3.76Å), alkyl interaction of terminal C from 4-Et with Ile-186 (5.32Å), carbon H-bond between C19 and Phe-226 (3.75Å) carbon H-bond between C20 and Asn-344 (3.70Å), π - π T shaped of ring B with Phe-340 (4.77Å), attractive charge interaction of N11 with Asp-135 (3.72Å), conventional H-bond between H21 and Ser-139 (2.10Å). <i>Intramolecular H-bond between H21 and O from 2-OH in ring B (2.17Å).</i>
19	π - π T shaped of ring A with Phe-341 (5.19Å), π - π stacking of ring A with Phe-217 (5.48Å), π -alkyl of ring A with Val-136 (5.18Å), π - σ of terminal C from 4-Et with Phe-217 (3.57Å), π -anion of ring B with Asp-135 (4.67Å), π -alkyl of ring B with Val-136 (5.03Å) and Leu-132 (5.25Å), π -cation of N11 with Phe-340 (4.75Å), unfavorable donor-donor interaction of H21 with Ser-139 (1.39Å).
20	π - π T shaped of ring A with Phe-340 (4.67Å), π -alkyl of ring A with Val-136 (4.79Å), π -alkyl of terminal C from 4-Et with Phe-340 (4.97Å), Tyr-370 (4.21Å) and Trp-337 (4.96Å), alkyl interaction of terminal C from 4-Et with Val-366 (3.64Å), π - π stacking of ring B with Phe-217 (5.08Å), π - π stacking of methylenedioxy moiety with Phe-217 (4.03Å), π - σ of ring B with Ser-222 (3.76Å).
21+	π - π T shaped of ring A with Phe-341 (4.98Å), π -alkyl of ring A with Val-136 (4.87Å), π - σ of terminal C from 4-Pr with Phe-217 (3.95Å), alkyl interaction of terminal C from 4-Pr with Ile-186 (5.26Å), carbon H-bond between C20 and Asn-344 (3.37Å), π -alkyl of ring B with Val-136 (5.20Å) and Leu-209 (4.88Å), π - σ of ring B with Leu-132 (3.70Å), salt bridge between H21 and Asp-135 (2.48Å). <i>Intramolecular H-bond between H21 and O from 2-OMe in ring B (2.79Å).</i>
22	π - π T shaped of ring A with Phe-340 (4.67Å), π - σ of ring A with Val-136 (3.90Å), π -alkyl of terminal C from 4-Pr with Phe-340 (4.22Å), Tyr-370 (5.19Å) and Trp-337 (5.19Å), alkyl interaction of terminal C from 4-Pr with Val-366 (3.77Å), π - π T shaped of ring B with Phe-341 (5.00Å), π -alkyl of ring B with Ile-186 (5.19Å), π -cation of N11 with Phe-217 (4.68Å).
23#	π - π T shaped of ring A with Phe-341 (5.01Å), π -alkyl of ring A with Val-136 (4.93Å), π - σ of terminal C from 4-Pr with Phe-217 (3.75Å), carbon H-bond between C19 and Phe-226 (3.78Å), π -anion of ring B with Asp-135 (3.42Å), π -alkyl of ring B with Val-136 (4.83Å), attractive charge interaction of N11 with Asp-135 (3.82Å), π -cation of N11 with Phe-340 (4.90Å), conventional H-bond between H21 and Ser-139 (2.75Å). <i>Intramolecular π-σ interaction of C20 with ring B (3.59Å).</i>
24	π - π T shaped of ring A with Phe-341 (5.21Å), π - σ of ring A with Val-136 (3.58Å), π - π stacking of ring A with Phe-217 (5.80Å), alkyl interaction of terminal C from 4-Pr with Ile-186 (4.17Å), unfavorable acceptor-acceptor interaction of O8 with Ser-139 (2.92Å), π -alkyl of ring B with Val-136 (4.68Å) and Leu-132 (4.93Å), π - σ of ring B with Val-209 (3.62Å), π -alkyl of methylenedioxy moiety with Val-209 (5.11Å).
25+	π -alkyl of ring A with Val-366 (4.63Å), π -sulfur of S in 4-SMe of ring A with Trp-131 (5.36Å), alkyl interaction of C in 4-SMe with Val-208 (5.26Å), carbon H-bond between C20 and Glu-363 (3.56Å), π - σ of ring B with Val-136 (3.66Å), π - π T shaped of ring B with Phe-341 (5.66Å), attractive charge interaction of N11 with Asp-135 (5.01Å). <i>Intramolecular H-bond between H21 and O from 2-OMe in ring B (2.29Å).</i>
26	π - π T shaped of ring A with Phe-341 (5.17Å), π -alkyl of ring A with Val-136 (4.54Å), π - π stacking of ring A with Phe-217 (5.56Å), π -sulfur of S from 4-SMe with Phe-217 (4.00Å), π -alkyl of C from 4-SMe with Phe-217 (4.29Å), alkyl interaction of C from 4-SMe with Ile-186 (5.24Å), carbon H-bond between C20 and Asn-344 (3.56Å), π -alkyl of ring B with Val-366 (5.00Å), unfavorable acceptor-acceptor of O from 2-OH in ring B with Tyr-370 (2.97Å), salt bridge of H21 with Asp-135 (2.22Å).
27	π - π T shaped of ring A with Phe-341 (5.15Å), π - σ of ring A with Val-136 (3.55Å), π -alkyl of C in 4-SMe with Phe-217 (4.32Å), carbon H-bond between C20 and Asn-344 (3.70Å), π -alkyl of ring B with Leu-132 (5.13Å), salt bridge between H21 and Asp-135 (2.33Å).
28*	π - π T shaped of ring A with Phe-341 (5.00Å), π -alkyl of ring A with Val-136 (4.78Å), π - σ of C in 4-SMe with Phe-217 (3.82Å), alkyl interaction of C in 4-SMe with Ile-186 (5.36Å), carbon H-bond between C20 and Phe-226 (3.67Å), carbon H-bond between C19 and Asn-344 (3.58Å), π -alkyl of ring B with Val-136 (5.07Å), Leu-132 (5.13Å) and Leu-209 (5.00Å), π - π T shaped of methylenedioxy moiety with Phe-340 (5.31Å), salt bridge between H21 and Asp-135 (2.31Å). <i>Intramolecular π-π stacking of ring A with ring B (5.59Å).</i>
29	π - π T shaped of ring A with Phe-341 (5.03Å), π -alkyl of ring A with Val-136 (4.84Å), π - σ of C in 4-SMe with Phe-217 (3.54Å), carbon H-bond between C19 and Asn-344 (3.68Å), π -anion of ring B with Asp-135 (4.19Å), π -alkyl of ring B with Val-136 (4.86Å), Leu-132 (5.24Å) and Leu-209 (5.04Å), salt bridge between H21 and Asp-135 (2.18Å).
30^	π - π T shaped of ring A with Phe-341 (5.03Å), π - σ of ring A with Val-136 (3.74Å), π -sulfur of S from 4-SEt in ring A with Phe-217 (4.44Å), π - σ of terminal C from 4-SEt with Phe-217 (3.69Å), carbon H-bond between C19 and Phe-226 (3.75Å), π - π T shaped of ring B with Phe-340 (4.83Å), π -alkyl of ring B with Val-366 (5.17Å), carbon H-bond between C12 and Asp-135 (3.34Å), attractive charge interaction of N11 and Asp-135 (3.78Å), conventional H-bond between H from 2-OH in ring B and Asp-135 (2.75Å). <i>Intramolecular unfavorable donor-donor interaction of H21 and H from 2-OH (1.70Å).</i>
31+	π - π T shaped of ring A with Phe-340 (5.24Å), π -alkyl of terminal C from 4-SEt with Phe-340 (4.74Å), alkyl interaction of terminal C from 4-SEt with Val-366 (4.60Å) and Leu-362 (3.95Å), conventional H-bond between O8 and Tyr-370 (2.66Å), carbon H-bond

	between C19 and Asp-135 (3.54Å), π - π T shaped of ring B with Phe-341 (4.83Å), π -alkyl of ring B with Val-136 (5.37Å), carbon H-bond between F and Ser-139 (3.35Å), π -cation of N11 with Phe-340 (4.71Å). <i>Intramolecular H-bond between O7 and H21</i> (2.53Å).
32	π - π T shaped of ring A with Phe-341 (5.14Å), π -alkyl of ring A with Val-136 (4.62Å), π - π stacking of ring A with Phe-217 (5.61Å), π -sulfur of S from 4-SEt with Phe-341 (5.27Å), π - σ of C19 with Phe-217 (3.17Å), alkyl interaction of terminal C from 4-SEt with Ile-186 (4.17Å), π - σ of ring B with Leu-362 (3.92Å), π -alkyl of methylenedioxy moiety with Val-208 (5.13Å) and Met-218 (5.36Å), conventional H-bond between O from methylenedioxy moiety and Gln-359 (2.16Å).
33	π - π T shaped of ring A with Phe-340 (5.08Å), π - σ of ring A with Val-136(3.59Å), π -sulfur of S from 4-SPr with Phe-340 (5.27Å), π -alkyl of terminal C from 4-SPr with Phe-217 (4.25Å), alkyl interaction of terminal C from 4-SPr with Val-136 (5.09Å), π -alkyl of ring B with Leu-132 (5.32Å), salt bridge between H21 and Asp-135 (2.82Å).
34*+	π - σ of ring A with Val-366 (3.38Å), π -sulfur of S from 4-SPr with Phe-340 (5.17Å), π -alkyl of terminal C from 4-SPr with Phe-340 (5.16Å), alkyl interaction of terminal C from 4-SPr with Val-136 (4.43Å), carbon H-bond between C20 and Asn-344 (3.57Å), π - σ of ring B with Val-208 (3.65Å and 3.82Å), salt bridge between H21 and Glu-363 (2.53Å). <i>Intramolecular H-bond between H21 and O7</i> (2.31Å), <i>intramolecular π-π stacking of ring A with ring B</i> .
35+	π - π T shaped of ring A with Phe-341 (5.24Å), π - σ of ring A with Val-136 (3.88Å), π -alkyl of terminal C from 4-SPr with Phe-217 (4.11Å), π -anion of ring B with Asp-135 (3.41Å), π -alkyl of ring B with Val-366 (5.17Å), π - π stacking of ring A with Phe-340 (5.29Å), π -cation of N11 with Phe-340 (4.03Å), attractive charge interaction of N11 with Asp-135 (5.09Å). <i>Intramolecular H-bond between H21 and O7</i> (2.32Å).
36**#	π - σ of ring A with Leu-132 (3.97Å), π -alkyl of ring A with Leu-209 (5.44Å), alkyl interaction of terminal C from 4-SPr with Val-366 (4.53Å) and Ala-111 (3.51Å), π -alkyl of terminal C from 4-SPr and Trp-367 (4.78Å and 5.48Å), π -alkyl of ring B with Val-366 (5.22Å), π - σ of ring B with Leu-362 (3.90Å), π -alkyl of methylenedioxy moiety with Leu-362 (5.31Å), unfavorable positive-positive interaction of N11 with Lys-211 (3.46Å), unfavorable donor-donor interaction of H21 with Lys-211 (1.81Å). <i>Intramolecular π-π stacking of ring A with ring B</i> (4.12Å), <i>methylenedioxy moiety</i> (5.30Å), <i>intramolecular π-σ interaction of C20 with methylenedioxy moiety</i> (3.73Å).
37	π - π T shaped of ring A with Phe-341 (5.21Å), π - σ of ring A with Val-136 (3.68Å), π -alkyl of C from 4-CF ₃ with Phe-341 (4.84Å), alkyl interaction of C from 4-CF ₃ with Ile-186 (5.25Å), conventional H-bond between O7 and Ser-139 (2.66Å), π -alkyl of ring B with Leu-209 (3.98Å), π -sulfur of ring B with Met-218 (5.37Å).
38**+	π -alkyl of ring A with Val-136 (4.91Å), π -alkyl of C from 4-CF ₃ with Phe-217 (4.05Å), halogen interaction of one F from 4-CF ₃ with Ile-186 (3.58Å), halogen interaction of one F from 4-CF ₃ with Phe-220 (3.34Å), π -alkyl of ring B with Val-136 (5.04Å), Leu-132 (5.32Å) and Leu-209 (5.19Å), salt bridge between one H from N11 and Asp-135 (3.15Å). <i>Intramolecular π-π stacking of ring A with ring B</i> (5.72Å), <i>intramolecular π-σ interaction of ring B with C19</i> (3.71Å), <i>intramolecular H-bond between O7 and H21</i> (3.04Å).
39*+	π - π T shaped of ring A with Trp-131 (5.13Å), π -alkyl of C from 4-CF ₃ with Trp-131 (5.27Å), H-bond between one F from 4-CF ₃ and Tyr-370 (2.16Å), halogen interaction of one F from 4-CF ₃ with Ala-111 (3.65Å) and another F from 4-CF ₃ with Glu-363 (3.02Å), alkyl interaction of C from 4-CF ₃ with Val-366 (4.30Å) and Ala-111 (4.12Å), carbon H-bond between C20 and Cys-207 (3.53Å), π -alkyl of ring B with Val-366 (5.17Å). <i>Intramolecular π-π stacking of ring A with ring B</i> (3.76Å), <i>intramolecular carbon H-bond between C19 and F in ring B</i> (3.39Å).
40###+	π -alkyl of ring A with Val-136 (4.94Å), π -alkyl of C from CF ₃ with Phe-217 (4.05Å), halogen interaction of F from 4-CF ₃ with Phe-220 (3.46Å), π -alkyl of ring B with Val-136 (4.92Å), Leu-132 (4.70Å) and Leu-209 (5.15Å), carbon H-bond between C10 and Ser-139 (3.54Å). <i>Intramolecular π-σ interaction of ring B with C19</i> (3.73Å), <i>intramolecular π-σ interaction of methylenedioxy moiety with C19</i> (3.84Å), <i>intramolecular H-bond between O7 and H21</i> (2.28Å).
41*#	π - π T shaped of ring A with Phe-341 (5.13Å), π -alkyl of ring A with Val-136 (4.94Å), π - π stacking of ring A with Phe-217 (5.58Å), carbon H-bond between C20 and Asn-344 (3.49Å), carbon H-bond between N from 4-CN with Phe-220 (3.78Å), π -alkyl of ring B with Val-136 (4.76Å), π - σ of ring B with Leu-132 (3.82Å), conventional H-bond between H21 and Ser-139 (2.55Å). <i>Intramolecular π-π stacking of ring A with ring B</i> (5.25Å), <i>intramolecular π-σ interaction of C20 with ring B</i> (3.59Å).
42	π - π T shaped of ring A with Phe-341 (5.06Å), π -alkyl of ring A with Val-136 (4.96Å), carbon H-bond between C20 and Asn-344 (3.63Å), π -alkyl of ring B with Val-366 (5.05Å), conventional H-bond between H from 2-OH in ring B and Tyr-370 (2.31Å) and Asp-135 (2.90Å), salt bridge between H21 and Asp-135 (2.18Å), conventional H-bond between H21 and Ser-139 (2.53Å).
43	π - π T shaped of ring A with Phe-341 (5.38Å), π -alkyl of ring A with Ile-186 (4.80Å), conventional H-bond of N from 4-CN and Trp-144 (2.71Å), π - σ of ring B with Val-136 (3.49Å).
44*#	π - π T shaped of ring A with Phe-341 (5.18Å), π -alkyl of ring A with Val-136 (5.07Å), π - π stacking of ring A with Phe-217 (5.48Å), carbon H-bond between C20 and Asn-344 (3.45Å), carbon H-bond between N from 4-CN with Phe-220 (3.80Å), conventional H-bond between O7 and Thr-140 (2.04Å), π -alkyl of ring B with Leu-209 (5.41Å) and Leu-132 (4.96Å), salt bridge between H21 and Asp-135 (3.14Å). <i>Intramolecular π-π stacking of ring A with ring B</i> (5.51Å), <i>intramolecular π-σ interaction of C20 with ring B</i> (3.69Å).

*Intramolecular interactions: *: π - π stacking, +: H-bond (any kind), #: π - σ interaction, ^: unfavorable interactions.*

DISCUSSION

Local MO structure

In the case of O7 and O8 (Table 2, Fig. 2) the local (HOMO)* coincides with the molecular HOMO in all molecules. (HOMO)* and (HOMO-1)* are of π nature and (HOMO-2)* can be of σ or π nature. The first vacant local MO of these atoms corresponds, in all molecules, to the molecular (LUMO+4) and it has a π nature. This MO is followed by two vacant MOs of σ nature. In the case of C19 and C20 (the carbon atoms of the OMe substituents, Table 2 and Fig. 2) all MOs are of σ nature. The local frontier MOs (HOMO* and LUMO*) do not correspond to the molecular frontier MOs. In some cases LUMO* and (LUMO+1)* are energetically close and in others the (LUMO+1)* energy is relatively far from the LUMO* energy. In the case of the carbon atoms of ring B (C14, C15 and C18, Tables 2 and 3, Fig. 2) the local HOMO* is energetically close to the molecule's HOMO. The (HOMO-1)* can be of π or σ nature. In the majority of cases (HOMO-2)* is of σ nature and it is energetically far from (HOMO-1)*. If (HOMO-2)* is of π nature it is energetically close to (HOMO-1)*. In all cases the first vacant local MO, LUMO*, coincides with the molecular LUMO and it is of π nature. In all cases but three, (LUMO+1)* coincides with LUMO.

LMRA results

To interpret the results we must understand that it is the *simultaneous* variation of the numerical values of the LARIs appearing in the equations which explains the variation of the binding affinity throughout the group of molecules. All molecular orbital-related LARIs used here (Fukui indices and orbital superdelocalizabilities) have non-zero values (this is so because of the way we build the data matrix, see [58, 76] for details). Then, it is reasonable to admit that if, for example, an occupied MO different from the HOMO and localized on a certain atom appears in the equations, the occupied MOs having a lower energy and localized on the same atom also take part in the interaction. The analysis is carried out employing the *variable-by-variable* (VbV) approach: the condition that a single reactivity index must fulfill for a high pK_i is determined and the corresponding interaction or interactions are suggested. In the case of the MO-related LARIs the nature (σ or π) of the MOs must be taken into account.

5-HT_{2B} receptor binding affinity of the whole set of molecules (set I).

The beta values (Table 4) show that the importance of the variables in Eq. 2 is $\omega_{12} > Q_3 > S_{19}^E(HOMO-2)^* > s_6 > F_7(LUMO+2)^* > F_{20}(LUMO+1)^* > S_{15}^E(HOMO)^* > Q_9^{\max}$. Q_9^{\max} will not be discussed because of its high p value. A small value for ω_{12} (see Fig. 2 for atom numbering) is required for high receptor binding affinity. Atom 12 is a carbon linking the NH₂ group with ring B. The local atomic electrophilicity of atom 12 is defined as [59]:

$$\omega_{12} = \frac{\mu_{12}^2}{2\eta_{12}} \quad (5)$$

where μ_{12} is the local atomic electronic chemical potential of atom 12 (its tendency to receive charge, the $(HOMO)_{12}^* - (LUMO)_{12}^*$ midpoint) and η_{12} its local atomic hardness (resistance to exchange charge with the medium, the $(HOMO)_{12}^* - (LUMO)_{12}^*$ distance). As atom 12 must have a low electrophilicity we state that in this atom the $(HOMO)_{12}^* - (LUMO)_{12}^*$ distance should be as great as possible while the $(HOMO)_{12}^* - (LUMO)_{12}^*$ midpoint should be displaced upwards in the energy axis (if μ_{12} is negative). For these reasons we suggest that atom 12 interacts as an electron-donor center. Possible interactions are alkyl-alkyl and/or π -alkyl. Q_3 should be as negative as possible. Being atom 3 a carbon of ring A, the net charge will be controlled by the nature of the substituent at position 2 (this is the only position with different substitutions in this ring, see Fig. 2). Atom 3 could participate in (favorable) anion-cation or anion- π interactions. A possible π - π interaction including atoms 3 and 6 is not ruled out. Atom 6 is a carbon belonging to ring A (Fig. 2). A small value for s_6 is associated with high affinity. As this local atomic reactivity index is defined as the inverse of the $(HOMO)_6^* - (LUMO)_6^*$ distance [59], a large value for this distance is required. This can be obtained by raising the $(LUMO)_6^*$ energy. Within this condition, atom 6 will act as an electron-donor center and participate in, for example, a π - π stacking interaction. Atom 19 is a carbon of the 2-OMe substituent (position 6 in Fig. 2). $(HOMO-2)_{19}^*$ is a MO of σ nature (Table 3). A small value of $S_{19}^E(HOMO-2)^*$ suggests that this MO is engaged in a repulsive interaction with occupied MOs of a moiety of the binding site. It also suggests that $(HOMO-1)_{19}^*$ and $(HOMO)_{19}^*$ could be engaged in alkyl-alkyl and/or π -alkyl interactions. Atom 20 is a carbon of the 5-OMe substituent (position 3 in Fig. 2). $(LUMO+1)_{20}^*$ is a σ MO (Table 3). A small value for $F_{20}(LUMO+1)^*$ suggests that a high receptor affinity is related to a low electron population on this atom. It is probable then that atom 20 is engaged in alkyl-alkyl and/or π -alkyl interactions acting as an electron-deficient center. Atom 7 is the oxygen of the 2-OMe substituent. $(LUMO+2)_7^*$ is a σ MO (Table 2). A high value for $F_7(LUMO+2)^*$ indicates that the first three lowest vacant MOs seem to interact with one or more electron-rich centers. The reason for this suggestion is that $(LUMO)_7^*$ is a π MO while $(LUMO+1)_7^*$ can be of π or σ nature (Table 2). Atom 15 is a carbon belonging to ring B. $(HOMO)_{15}^*$ is a π MO (Table 2). A low value for $S_{15}^E(HOMO)^*$ can be associated with a low electron-donor capacity of atom 15. Therefore, it is suggested that atom 15 interacts with a rich-electron center via π - π stacking involving more carbon atoms of ring B. All these ideas are summarized in the partial two-dimensional (2D) pharmacophore shown in Fig. 17.

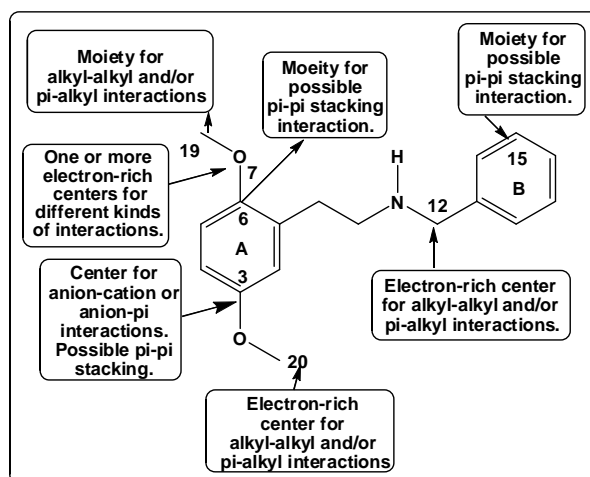


Figure 17. Partial 2D pharmacophore for the interaction of group I of molecules with the 5-HT_{2B} receptor

5-HT_{2B} receptor binding affinity of set II

The beta values (Table 6) show that the importance of the variables in Eq. 3 is $F_{20}(HOMO-1)^* > S_{15}^E(HOMO-2)^* > S_8^E(HOMO-2)^* > S_{18}^E(HOMO)^*$. Atom 20 is the carbon atom of the 5-OMe substituent of ring A (Fig. 2). $(HOMO-1)_{20}^*$ is a σ MO. A small value for $F_{20}(HOMO-1)^*$ suggests that it is engaged in a unfavorable interaction and that probably only $(HOMO)_{20}^*$ participates in alkyl-alkyl and/or alkyl- π interactions. Atom 8 is the oxygen atom of the 2-OMe substituent of ring A. $(HOMO-2)_8^*$ is a σ MO. A high value for $S_8^E(HOMO-2)^*$ indicates that the corresponding MO is interacting with an electron-deficient moiety probably through a σ - π interaction. $(HOMO-1)_8^*$ and $(HOMO)_8^*$, both of π nature can be participating in π - π and/or π -cation interactions. Atoms 15 and 18 are carbon atoms belonging to B ring. The ring is probably engaged in π - π (stacked or T-shaped) or π -atom interactions. A small value for $S_{18}^E(HOMO)^*$ indicates that $(HOMO)_{18}^*$ is facing an electron-rich center available for π - π and/or π -anion interactions. The case of atom 15 is more complex. $(HOMO-2)_{15}^*$ and $(HOMO-1)_{15}^*$ are a σ or π MO while $(HOMO)_{15}^*$ is a π MO (Table 2). Then atom 15 can participate in a π - π interaction but also in atom-atom interactions. The above suggestions are depicted in the partial 2D pharmacophore shown in Fig. 18.

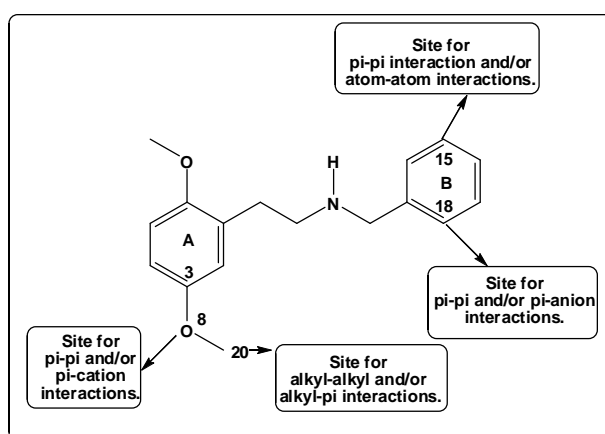


Figure 18. Partial 2D pharmacophore for the interaction of group II of molecules with the 5-HT_{2B} receptor

5-HT_{2B} receptor binding affinity of set III

The beta values (Table 8) show that the importance of the variables in Eq. 4 is $Q_{19} > Q_4 > Q_{21}^{\max} > S_{14}^E(HOMO-1)^* > S_7^N(LUMO+2)^* = F_{19}(LUMO+1)^* > S_8^N(LUMO+2)^*$.

Atom 19 is the carbon atom of the 2-OMe substituent of ring A (Fig. 2). Atom 19 should have a positive net charge for high affinity. Then, atom 19 should be engaged at least in a cation- π and/or cation-anion interactions (an unfavorable interaction with another positively-charged moiety cannot be excluded). Atom 4 is a carbon atom of ring A and should have a positive net charge, allowing an interaction with a negatively-charged moiety (carboxylate for example) and/or a cation- π interaction. Atom 21 is one of the hydrogen atoms bonded to N11 (Fig. 2). A small value of Q_{21}^{\max} is required for high receptor affinity. Q_{21}^{\max} is defined as [59]:

$$Q_{21}^{\max} = -\frac{\mu_{21}}{\eta_{21}} \quad (6)$$

Given that η_{21} corresponds to the $(HOMO)_{21}^* - (LUMO)_{21}^*$ distance and that μ_{21} is the midpoint between the frontier local MOs, a small value for Q_{21}^{\max} could be obtained with a large η_{21} value and/or with the shifting of μ_{21} upwards in the energy axis. Now, $(HOMO)_{21}^*$ of a hydrogen atom lay energetically very far below from the molecule's HOMO while $(LUMO)_{21}^*$ coincides with the molecule's LUMO. This suggests that atom 21 is a good electron-acceptor. This suggests the possibility of a hydrogen-bond and/or a charge-charge interaction. Atom 14 is a carbon belonging to ring B. $(HOMO-1)_{14}^*$ can be a π or σ MO (Table 3). $(HOMO)_{14}^*$ is a π MO. Then, a high value for $S_{14}^E(HOMO-1)^*$ is suggestive of π - π interactions (but without ruling out possible σ - π interactions). We know that nucleophilic superdelocalizabilities may have positive or negative values [59]. On the other hand they can be accompanied by positive or negative coefficients in LRMA equations. Atoms 7 and 8 are, respectively, the oxygen atoms of the 2- and 5-OMe substituents in ring A. With the above considerations we suggest that in the case of atom 7 $(LUMO+2)_7^*$ and $(LUMO+1)_7^*$ (a σ MOs, Table 2) could be engaged in σ - π interactions, while $(LUMO)_7^*$ can participate in π - π interactions. The case of atom 8 is slightly different: it seems to use only its first two lowest vacant MOs for similar interactions. Atom 19 is the carbon of the 2-OMe substituent of ring A. $(LUMO+1)_{19}^*$ is a σ MO and a high value for $F_{19}(LUMO+1)^*$ is required for high receptor affinity. We suggest that atom 19 is employing its first two lowest vacant MOs to interact with a moiety of the receptor. The interactions can be of σ - π or alkyl-alkyl kinds. This is consistent with a positive value for Q_{19} (see above). These interpretations are depicted in the partial 2D pharmacophore shown in Fig. 19.

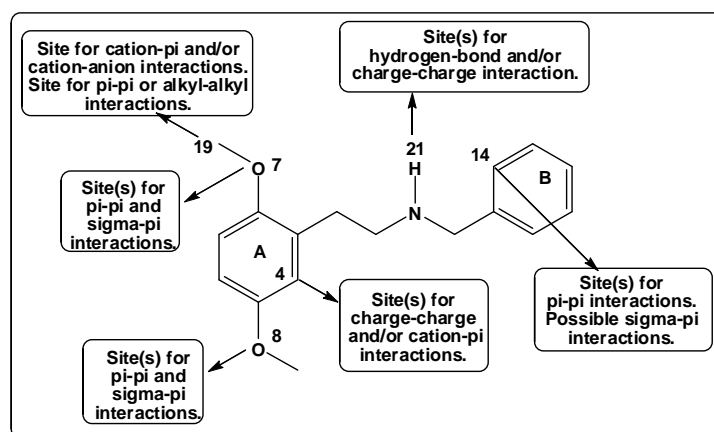


Figure 19. Partial 2D pharmacophore for the interaction of group III of molecules with the 5-HT_{2B} receptor

Docking results

First, it is interesting to note that with the use of Autodock 4 [107], and within the approximation of rigid residues (the residues of the active site were not allowed to change their conformation), we were able to find qualitative correlations between docking and quantum-chemical results [87, 101]. The discussion will be carried out on the basis of appropriate Tables built from Table 11 (see Fig. 2 for atom numbering). Despite the fact that no reactivity

index of the first atom of the 4-substituents of ring A appeared in the LMRA equations, docking results show several kinds of interactions displayed in Table 12.

Table 12. Intermolecular interactions of the 4-substituents of ring A

Mol.	Interactions
1	π -alkyl interaction of Br with Phe-341 (5.01Å), alkyl interaction of Br with Ile-186 (5.39Å).
2	π -alkyl interaction of Br with Phe-217 (4.06Å).
3	π -alkyl interaction of Br with Phe-217 (4.13Å).
4	π -alkyl interaction of Br with Trp-131 (4.90Å).
5	Alkyl interaction of Cl with Ile-186 (4.06Å).
6	Alkyl interaction of Cl with Leu-132 (4.47Å) and Leu-209 (3.79Å).
7	Alkyl interaction of Cl with Ile-186 (4.40Å) and Ala-224 (3.61Å), halogen interaction of Cl with Phe-220 (3.23Å).
8	Alkyl interaction of Cl with Ile-186 (4.78Å) and Ala-224 (4.20Å), halogen interaction of Cl with Ala-224 (3.23Å).
9	Halogen interaction of F with Phe-220 (3.36Å).
10	Halogen interaction of F with Phe-220 (3.45Å).
11	Halogen interaction of F with Ala-224 (3.30Å).
12	Carbon H-bond of F with Ala-224 (3.39Å).
13	π -alkyl interaction of C from 4-Me with Phe-341 (5.27Å).
14	π -alkyl interaction of C from 4-Me with Phe-217 (4.57Å).
15	π - σ interaction of C from 4-Me with Phe-217 (3.88Å).
16	Alkyl interaction of C from 4-Me with Ala-111 (4.46Å) and Val-366 (3.78Å).
17	π - σ interaction of terminal C from 4-Et with Phe-217 (3.56Å).
18	π - σ interaction of terminal C from 4-Et with Phe-217 (3.76Å), alkyl interaction of terminal C from 4-Et with Ile-186 (5.32Å).
19	π - σ interaction of terminal C from 4-Et with Phe-217 (3.57Å).
20	π -alkyl interaction of terminal C from 4-Et with Phe-340 (4.97Å), Tyr-370 (4.21Å) and Trp-337 (4.96Å), alkyl interaction of terminal C from 4-Et with Val-366 (3.64Å).
21	π - σ interaction of terminal C from 4-Pr with Phe-217 (3.95Å), alkyl interaction of terminal C from 4-Pr with Ile-186 (5.26Å).
22	π -alkyl interaction of terminal C from 4-Pr with Phe-340 (4.22Å), Tyr-370 (5.19Å) and Trp-337 (5.19Å), alkyl interaction of terminal C from 4-Pr with Val-366 (3.77Å).
23	π - σ interaction of terminal C from 4-Pr with Phe-217 (3.75Å).
24	Alkyl interaction of terminal C from 4-Pr with Ile-186 (4.17Å).
25	π -sulfur interaction of S in 4-SMe of ring A with Trp-131 (5.36Å), alkyl interaction of C in 4-SMe with Val-208 (5.26Å).
26	π -sulfur interaction of S from 4-SMe with Phe-217 (4.00Å), π -alkyl interaction of C from 4-SMe with Phe-217 (4.29Å), alkyl interaction of C from 4-SMe with Ile-186 (5.24Å).
27	π -alkyl interaction of C in 4-SMe with Phe-217 (4.32Å).
28	π - σ interaction of C in 4-SMe with Phe-217 (3.82Å), alkyl interaction of C in 4-SMe with Ile-186 (5.36Å).
29	π - σ interaction of C in 4-SMe with Phe-217 (3.54Å).
30	π -sulfur interaction of S from 4-SEt in ring A with Phe-217 (4.44Å), π - σ of terminal C from 4-SEt with Phe-217 (3.69Å).
31	π -alkyl interaction of terminal C from 4-SEt with Phe-340 (4.74Å), alkyl interaction of terminal C from 4-SEt with Val-366 (4.60Å) and Leu-362 (3.95Å).
32	π -sulfur interaction of S from 4-SEt with Phe-341 (5.27Å), alkyl interaction of terminal C from 4-SEt with Ile-186 (4.17Å).
33	π -sulfur interaction of S from 4-SPr with Phe-340 (5.27Å), π -alkyl interaction of terminal C from 4-SPr with Phe-217 (4.25Å), alkyl interaction of terminal C from 4-SPr with Val-136 (5.09Å).
34	π -sulfur interaction of S from 4-SPr with Phe-340 (5.17Å), π -alkyl interaction of terminal C from 4-SPr with Phe-340 (5.16Å), alkyl interaction of terminal C from 4-SPr with Val-136 (4.43Å).
35	π -alkyl interaction of terminal C from 4-SPr with Phe-217 (4.11Å).
36	Alkyl interaction of terminal C from 4-SPr with Val-366 (4.53Å) and Ala-111 (3.51Å), π -alkyl interaction of terminal C from 4-SPr and Trp-367 (4.78Å and 5.48Å).
37	π -alkyl interaction of C from 4-CF ₃ with Phe-341 (4.84Å), alkyl interaction of C from 4-CF ₃ with Ile-186 (5.25Å).
38	π -alkyl interaction of C from 4-CF ₃ with Phe-217 (4.05Å), halogen interaction of one F from 4-CF ₃ with Ile-186 (3.58Å), halogen interaction of one F from 4-CF ₃ with Phe-220 (3.34Å).
39	π -alkyl interaction of C from 4-CF ₃ with Trp-131 (5.27Å), H-bond between one F from 4-CF ₃ and Tyr-370 (2.16Å), halogen interaction of one F from 4-CF ₃ with Ala-111 (3.65Å), halogen interaction of another F from 4-CF ₃ with Glu-363 (3.02Å), alkyl interaction of C from 4-CF ₃ with Val-366 (4.30Å) and Ala-111 (4.12Å).
40	π -alkyl interaction of C from 4-CF ₃ with Phe-217 (4.05Å), halogen interaction of F from 4-CF ₃ with Phe-220 (3.46Å).
41	Carbon H-bond between N from 4-CN with Phe-220 (3.78Å).
43	Conventional H-bond of N from 4-CN and Trp-144 (2.71Å).
44	Carbon H-bond between N from 4-CN with Phe-220 (3.80Å).

Table 12 shows that there are enough results indicating the participation of the 4-substituents of ring A in 5-HT_{2B} binding. Notice that similar interactions are not always with the same residue (compare molecules 1-4, 5-8 and 41-44 for example, see Figs. 6, 7 and 16), and that some substituents interact with more than one site (molecules 20, 22 and 39 for example, see Figs. 10, 11 and 15). The analysis of the interaction distances shows that some of them are relatively strong (in molecules 8, 17 and 29 for example, see Figs. 7, 10 and 13) while others are definitively weak (in molecules 1, 13 and 25 for example, see Figs. 7, 9 and 12). Another important information provided by Table 12 is that sometimes, in 4-substituents, the atoms interacting with the residues are not those directly attached to ring A. As the common skeleton included only the LARIs of only the atom directly attached to ring A, this is probably the reason why Eqs. 2-4 do not contain indices related to this substituent. As the importance of the 4-substituent cannot be dismissed we are developing an analysis allowing us to include all the atoms in substituents of different length.

Regarding intramolecular interactions, molecule 25 (Fig. 12) presents a weak π - σ interaction between atoms O7 and C12. This is probably a consequence of the H-bond between H21 and Asn-344. Molecule 7 (Fig. 7) has also a weak π - σ interaction, but between a fluorine atom of ring B and C20. Molecule 39 (Fig. 15) has also a weak π - σ interaction between a fluorine atom of ring B and C19. The partial folding produced by this interaction is not enough to produce a direct interaction between rings A and B. In molecule 8 there is an H-bond between H21 and the oxygen atom of the methylenedioxy moiety. An intramolecular hydrogen bond between H21 and the oxygen atom of the OMe substituent in ring B appears in molecules 9, 17, 18, 21 and 25 (see Figs. 8, 10, 11 and 12). A H21-O7 H-bond is formed in molecules 11, 16, 31, 35, 38 and 40 (see Figs. 8, 9, 13, 14 and 15). These interactions seem to be a byproduct of other interactions of these molecules with the receptor's residues. If we consider the docking results as being more or less true for all molecules, then we can make a qualitative association with the results of Eq. 4 (set III) showing that H21 can form hydrogen bonds. Eq. 4 cannot provide information about the nature of the sites for H-bond formation. Note also that Eq. 2 and 3 do not have terms related to H21. Molecule 30 is the only one presenting an unfavorable donor-donor interaction between H21 and the H atom of the OH substituent in ring B. This interaction seems to appear as a result of the H-bond formation between the H atom of the OH substituent in ring B with Asp-135, the attractive charge interaction between N11 and Asp-135 and a C12-Asp-135 interaction. A π - σ intramolecular interaction occurs between C20 and ring B in molecules 3, 23, 38, 40, 41 and 44 (see Figs. 6, 11, 15 and 16). A π - σ intramolecular interaction also occurs between C20 and the methylenedioxy moiety in molecules 4, 36 and 40 (see Figs. 6, 14, and 15). In all but three cases (3, 23 and 40, see Figs. 6, 11 and 15) these kinds of interactions appear in molecules having an interaction between A and B rings. A direct π - π stacking interaction between rings A and B occurs in molecules 16, 28, 34, 36, 38, 39, 41 and 44 (see Figs. 9, 12, 14, 15 and 16). Molecules 16 and 38 show also a direct π - π stacking interaction between ring A and the methylenedioxy moiety. These interactions fold the molecules. The interaction of ring A with the site's residues is shown in Table 13.

Table 13. Intermolecular interactions of rings A and B with the 5-HT_{2B} site

Mol.	Interactions
1	π - π T shaped interaction of ring A with Phe-340 (5.44Å) and Phe-341(5.34Å), π - σ interaction of ring A with Val-136 (3.87Å), π - π T shaped interaction of ring B with Phe-340 (5.64Å), π -alkyl interaction of ring B with Val-366 (5.40Å) and Leu-362 (4.43Å).
2	π - π stacking interaction of ring A with Phe-217 (5.26Å), π -alkyl interaction of ring A with Val-136 (4.99Å), π - π T shaped interaction of ring B with Phe-340 (4.75Å), π - π stacking interaction of ring B with Trp-337 (4.19Å), π - σ interaction of ring B with Val-366 (3.78Å).
3	π - π T shaped interaction of ring A with Phe-341 (4.99Å), π -alkyl interaction of ring A with Val-136 (4.87Å), π -alkyl interaction of ring B with Val-136 (4.85Å), π -anion interaction between ring B and Asp-135 (3.88Å).
4	π -anion interaction of ring A with Glu-363 (4.01Å), π -alkyl interaction of ring B with Val-208 (5.49Å), π -alkyl interaction of methylenedioxy moiety with Val-366 (5.10Å).
5	π -alkyl interaction of ring A with Val-136 (5.17Å), π - π stacking interaction of ring B and Phe-340 (4.17Å), π -alkyl interaction of ring B and Val-366 (5.09Å).
6	π - π stacking interaction of ring B with Trp-131 (4.38Å).
7	π - π T shaped interaction of ring A with Phe-341 (5.36Å), π -alkyl interaction of ring A with Ile-186 (4.82Å), π - σ interaction of ring B and Val-136 (3.48Å).
8	π - π T shaped interaction of ring A with Phe-341 (4.76Å), π - σ interaction of ring B and Leu-132 (3.89Å), π -alkyl interaction of ring B and Val-136 (4.83Å), π -anion interaction of methylenedioxy moiety and Asp-135 (3.71Å), π - π T shaped interaction of methylenedioxy moiety and Phe-340 (5.26Å), π -alkyl interaction of methylenedioxy moiety with Val-366 (4.96Å).
9	π - σ interaction of ring A with Ser-222 (3.99Å), π -alkyl interaction of ring A with Ile-186 (4.78Å), π - σ interaction of ring B with Val-136 (3.51Å).
10	π - π T shaped interaction of ring A with Phe-341 (5.43Å), π -alkyl interaction of ring A with Ile-186 (4.80Å), π - σ interaction of ring B with Val-136 (3.58Å).
11	π - π T shaped interaction of ring A with Phe-341 (4.95Å), π -alkyl interaction of ring A with Ile-186 (5.26Å), π - π stacking interaction of ring B with Phe-340 (5.25Å), π -anion interaction of ring B with Asp-135 (3.49Å), π -alkyl interaction of ring B with Val-136 (5.34Å).
12	π - π T shaped interaction of ring A with Phe-341 (4.75Å), π - π T shaped interaction of methylenedioxy moiety and Phe-340 (5.48Å), π -anion interaction of methylenedioxy moiety and Asp-135 (3.91Å), π -alkyl interaction of ring B with Val-136 (4.89Å) and Leu-132 (4.93Å).
13	π - π T shaped interaction of ring A with Phe-341 (4.94Å), π -alkyl interaction of ring A with Val-136 (5.18Å), π -alkyl interaction of ring B with Val-208 (5.05Å) and Leu-209 (4.56Å).
14	π - π T shaped interaction of ring A with Phe-341 (5.07Å), π - π stacking interaction of ring A with Phe-217 (5.99Å), π -alkyl interaction of ring A with Val-136 (4.70Å), π -alkyl interaction of ring B with Val-136 (5.28Å) and Leu-209 (4.92Å), π - σ interaction of ring B with Leu-132 (3.72Å).
15	π - π stacking interaction of ring A with Phe-217 (5.28Å), π -alkyl interaction of ring A with Val-136 (5.24Å), π - π stacking interaction of ring B with Phe-340 (5.29Å), π -alkyl interaction of ring B with Val-136 (5.40Å), π -anion interaction of ring B with Asp-135 (3.33Å).
16	π - π T shaped interaction of ring A with Trp-131 (5.62Å), π -alkyl interaction of ring B with Val-366 (4.90Å) and Leu-362 (4.39Å), π -alkyl interaction of methylenedioxy moiety with Val-208 (5.23Å).
17	π - π T shaped interaction of ring A with Phe-341 (5.42Å), π -alkyl interaction of ring A with Val-136 (5.31Å), π - π interaction stacking of ring A with Phe-217 (5.30Å), π -anion interaction of ring B with Asp-135 (3.97Å).
18	π - π T shaped interaction of ring A with Phe-341 (5.08Å), π -alkyl interaction of ring A with Val-136 (4.47Å), π - π T shaped interaction of ring B with Phe-340 (4.77Å).
19	π - π T shaped interaction of ring A with Phe-341 (5.19Å), π - π stacking interaction of ring A with Phe-217 (5.48Å), π -alkyl interaction of ring A with Val-136 (5.18Å), π -anion interaction of ring B with Asp-135 (4.67Å), π -alkyl interaction of ring B with Val-136 (5.03Å) and Leu-132 (5.25Å).
20	π - π T shaped interaction of ring A with Phe-340 (4.67Å), π -alkyl interaction of ring A with Val-136 (4.79Å), π - π stacking interaction of

	ring B with Phe217 (5.08Å), π - π stacking interaction of methylenedioxy moiety with Phe-217 (4.03Å), π - σ interaction of ring B with Ser-222 (3.76Å).
21	π - π T shaped interaction of ring A with Phe-341 (4.98Å), π -alkyl interaction of ring A with Val-136 (4.87Å), π -alkyl interaction of ring B with Val-136 (5.20Å) and Leu-209(4.88Å), π - σ interaction of ring B with Leu-132 (3.70Å).
22	π - π T shaped interaction of ring A with Phe-340 (4.67Å), π - σ interaction of ring A with Val-136 (3.90Å), π - π T shaped interaction of ring B with Phe-341 (5.00Å), π -alkyl interaction of ring B with Ile-186 (5.19Å).
23	π - π T shaped interaction of ring A with Phe-341 (5.01Å), π -alkyl interaction of ring A with Val-136 (4.93Å), π -anion interaction of ring B with Asp-135 (3.42Å), π -alkyl interaction of ring B with Val-136 (4.83Å).
24	π - π T shaped interaction of ring A with Phe-341 (5.21Å), π - σ interaction of ring A with Val-136 (3.58Å), π - π stacking interaction of ring A with Phe-217 (5.80Å), π -alkyl interaction of ring B with Val-136 (4.68Å) and Leu-132 (4.93Å), π - σ interaction of ring B with Val-209 (3.62Å), π -alkyl interaction of methylenedioxy moiety with Val-209 (5.11Å).
25	π -alkyl interaction of ring A with Val-366 (4.63Å), π - σ interaction of ring B with Val-136 (3.66Å), π - π T shaped interaction of ring B with Phe-341 (5.66Å).
26	π - π T shaped interaction of ring A with Phe-341 (5.17Å), π -alkyl interaction of ring A with Val-136 (4.54Å), π - π stacking interaction of ring A with Phe-217 (5.56Å), π -alkyl interaction of ring B with Val-366 (5.00Å).
27	π - π T shaped interaction of ring A with Phe-341 (5.15Å), π - σ interaction of ring A with Val-136 (3.55Å), π -alkyl interaction of ring B with Leu-132 (5.13Å).
28	π - π T shaped interaction of ring A with Phe-341 (5.00Å), π -alkyl interaction of ring A with Val-136 (4.78Å), π -alkyl interaction of ring B with Val-136 (5.07Å), Leu-132 (5.13Å) and Leu-209 (5.00Å), π - π T shaped interaction of methylenedioxy moiety with Phe-340 (5.31Å).
29	π - π T shaped interaction of ring A with Phe-341 (5.03Å), π -alkyl interaction of ring A with Val-136 (4.84Å), π -anion interaction of ring B with Asp-135 (4.19Å), π -alkyl interaction of ring B with Val-136 (4.86Å), Leu-132 (5.24Å) and Leu-209 (5.04Å).
30	π - π T shaped interaction of ring A with Phe-341 (5.03Å), π - σ interaction of ring A with Val-136 (3.74Å), π - π T shaped interaction of ring B with Phe-340 (4.83Å), π -alkyl interaction of ring B with Val-366 (5.17Å).
31	π - π T shaped interaction of ring A with Phe-340 (5.24Å), π - π T shaped interaction of ring B with Phe-341 (4.83Å), π -alkyl interaction of ring B with Val-136 (5.37Å).
32	π - π T shaped interaction of ring A with Phe-341 (5.14Å), π -alkyl interaction of ring A with Val-136 (4.62Å), π - π stacking interaction of ring A with Phe-217 (5.61Å), π - σ interaction of ring B with Leu-362 (3.92Å), π -alkyl interaction of methylenedioxy moiety with Val-208 (5.13Å) and Met-218 (5.36Å).
33	π - π T shaped interaction of ring A with Phe-340 (5.08Å), π - σ interaction of ring A with Val-136(3.59Å), π -alkyl interaction of ring B with Leu-132 (5.32Å).
34	π - σ interaction of ring A with Val-366 (3.38Å), π - σ interaction of ring B with Val-208 (3.65Å and 3.82Å).
35	π - π T shaped interaction of ring A with Phe-341 (5.24Å), π - σ interaction of ring A with Val-136 (3.88Å), π -alkyl interaction of ring B with Val-366 (5.17Å), π - π stacking interaction of ring A with Phe-340 (5.29Å).
36	π - σ interaction of ring A with Leu-132 (3.97Å), π -alkyl interaction of ring A with Leu-209 (5.44Å), π -alkyl interaction of ring B with Val-366 (5.22Å), π - σ interaction of ring B with Leu-362 (3.90Å), π -alkyl interaction of methylenedioxy moiety with Leu-362 (5.31Å).
37	π - π T shaped interaction of ring A with Phe-341 (5.21Å), π - σ interaction of ring A with Val-136 (3.68Å), π -alkyl interaction of ring B with Leu-209 (3.98Å), π -sulfur interaction of ring B with Met-218 (5.37Å).
38	π -alkyl interaction of ring A with Val-136 (4.91Å), π -alkyl interaction of ring B with Val-136 (5.04Å), Leu-132 (5.32Å) and Leu-209 (5.19Å).
39	π - π T shaped interaction of ring A with Trp-131 (5.13Å), π -alkyl interaction of ring B with Val-366 (5.17Å).
40	π -alkyl interaction of ring A with Val-136 (4.94Å), π -alkyl interaction of ring B with Val-136 (4.92Å), Leu-132 (4.70Å) and Leu-209 (5.15Å).
41	π - π T shaped interaction of ring A with Phe-341 (5.13Å), π -alkyl interaction of ring A with Val-136 (4.94Å), π - π stacking interaction of ring A with Phe-217 (5.58Å), π -alkyl interaction of ring B with Val-136 (4.76Å), π - σ interaction of ring B with Leu-132 (3.82Å).
42	π - π T shaped interaction of ring A with Phe-341 (5.06Å), π -alkyl interaction of ring A with Val-136 (4.96Å), π -alkyl interaction of ring B with Val-366 (5.05Å).
43	π - π T shaped interaction of ring A with Phe-341 (5.38Å), π -alkyl interaction of ring A with Ile-186 (4.80Å), π - σ interaction of ring B with Val-136 (3.49Å).
44	π - π T shaped interaction of ring A with Phe-341 (5.18Å), π -alkyl interaction of ring A with Val-136 (5.07Å), π - π stacking interaction of ring A with Phe-217 (5.48Å), π -alkyl interaction of ring B with Leu-209 (5.41Å) and Leu-132 (4.96Å).

We can see that ring A uses a mixture of π - π T-shaped, π -alkyl, π - π stacking, π - σ , π -anion interactions to bind the 5-HT_{2B} site. The π - σ and π -anion interactions are the strongest ones (see the interaction distances in the above Table). The LMRA equations are able to detect some of the atoms participating in these interactions and suggest their possible nature. The anion- π interaction is suggested in Fig. 17. For the moment, our model-based method cannot distinguish between π - π T-shaped and π - π stacking interactions. Ring B uses a mixture of π - π T-shaped, π -alkyl, π - σ , π -sulfur, π - π stacking and π -anion interactions. In some cases the methylenedioxy moiety participates in the binding through π -alkyl, π - π T-shaped, π - π stacking and π -anion interactions. Table 13 also shows that rings A and B can bind different numbers of residues in the binding site. The LMRA results strongly emphasize the role of the carbon and oxygen atoms of the 2- and 5-OMe substituents of ring A. Table 14 shows their interactions.

Table 14. Intermolecular interactions of atoms O7, O8, C19 and C20 with the 5-HT_{2B} receptor site

Mol.	Interactions
1	Carbon H-bond between C19 of 2-Ome from ring A with Asp-135 (3.63Å).
2	Carbon H-bond between C19 and Asn-344 (3.80Å).
4	Carbon H-bond between C20 and Glu-363 (3.61Å).
5	π - σ interaction of C19 with Phe-217 (3.55Å), conventional H-bond between O8 and Thr-140 (2.35Å).
6	Carbon H-bond between C19 and Gln-359 (3.61Å), carbon H-bond between C20 and the two oxygen atoms of Asp-135 (3.48Å and 3.68Å).
9	Conventional H-bond between O19 from 2-OMe in ring B and Ser-139 (2.05Å).
11	Carbon H-bond of O8 with Ala-224 (3.57Å).
13	Carbon H-bond of C20 with Asp-135 (3.49Å), π - σ interaction of C19 with Phe-217 (3.90Å).
14	Carbon H-bond between C20 and Asn-344 (3.62Å).
15	Carbon H-bond between C20 and Asn-344 (3.74Å).
17	Conventional H-bond between O7 and Thr-140 (2.14Å), conventional H-bond between O8 and Asn-344 (2.61Å).
18	Carbon H-bond between C19 and Phe-226 (3.75Å), carbon H-bond between C20 and Asn-344 (3.70Å).
21	Carbon H-bond between C20 and Asn-344 (3.37Å).
23	Carbon H-bond between C19 and Phe-226 (3.78Å).
24	Unfavorable acceptor-acceptor interaction of O8 with Ser-139 (2.92Å).
25	Carbon H-bond between C20 and Glu-363 (3.56Å).
26	Carbon H-bond between C20 and Asn-344 (3.56Å).
27	Carbon H-bond between C20 and Asn-344 (3.70Å).
28	Carbon H-bond between C20 and Phe-226 (3.67Å), carbon H-bond between C19 and Asn-344 (3.58Å).
29	Carbon H-bond between C19 and Asn-344 (3.68Å).
30	Carbon H-bond between C19 and Phe-226 (3.75Å).
31	Conventional H-bond between O8 and Tyr-370 (2.66Å), carbon H-bond between C19 and Asp-135 (3.54Å).
32	π - σ interaction of C19 with Phe-217 (3.17Å).
34	Carbon H-bond between C20 and Asn-344 (3.57Å).
37	Conventional H-bond between O7 and Ser-139 (2.66Å).
39	Carbon H-bond between C20 and Cys-207 (3.53Å).
41	Carbon H-bond between C20 and Asn-344 (3.49Å).
42	Carbon H-bond between C20 and Asn-344 (3.63Å).
44	Carbon H-bond between C20 and Asn-344 (3.45Å), conventional H-bond between O7 and Thr-140 (2.04Å).

We may see that these four atoms are engaged, in some molecules, in different kinds of interactions with the 5-HT_{2B} receptor site. What we have called “carbon H-bond” refers to the interaction of a carbon donor atom and an acceptor (a non classical H-bond). Again, it is surprising that LRMA results show a qualitative correlation with docking results. As this is the first large scale comparison between a model-based model and docking results, it seems necessary to wait for more similar studies on other systems to begin to understand the relationships (that seem to exist) between the results of both models. It is absolutely necessary to employ docking methods allowing the change of conformation of the residues at the binding site: the results using rigid residues are entirely different and obviously do not reflect the real situation. LMRA results stress the role of H21 (see Fig. 2). Table 15 shows the H21 docking results.

Table 15. Intermolecular interactions of H21

Mol.	Interactions
1	Conventional H-bond between H21 and Asn-344 (2.01Å).
2	Salt bridge between H21 and Asp-135 (2.12Å).
3	Salt bridge between the two hydrogen atoms of N11 and Asp-135 (2.80Å and 3.00Å).
6	Salt bridge between H21 and Glu-363 (2.53Å).
13	Conventional H-bond between H21 and Asn-344 (2.36Å).
14	Salt bridge between H21 and Asp-135 (2.60Å).
17	Unfavorable donor-donor interaction of one H from N11 with Ser-139 (1.73Å).
18	Conventional H-bond between H21 and Ser-139 (2.10Å).
19	Unfavorable donor-donor interaction of H21 with Ser-139 (1.39Å).
21	Salt bridge between H21 and Asp-135 (2.48Å).
23	Conventional H-bond between H21 and Ser-139 (2.75Å).
26	Salt bridge of H21 with Asp-135 (2.22Å).
27	Salt bridge between H21 and Asp-135 (2.33Å).
28	Salt bridge between H21 and Asp-135 (2.31Å).
29	Salt bridge between H21 and Asp-135 (2.18Å).
33	Salt bridge between H21 and Asp-135 (2.82Å).
34	Salt bridge between H21 and Glu-363 (2.53Å).
36	Unfavorable donor-donor interaction of H21 with Lys-211 (1.81Å).
38	Salt bridge between H21 and Asp-135 (3.15Å).
41	Conventional H-bond between H21 and Ser-139 (2.55Å).
42	Salt bridge between H21 and Asp-135 (2.18Å), conventional H-bond between H21 and Ser-139 (2.53Å).
44	Salt bridge between H21 and Asp-135 (3.14Å).

We can see that atom H21 is involved in favorable H-bond interactions (molecules 17, 19 and 36 are exceptions, see Figs. 10 and 14) with Asp-135, Glu-363, Ser-139, Lys-111 and Asn-344. Ser-135 and Ser-139 seem to be the main targets (by "salt bridge" we mean hydrogen bonds between charged groups). Again there is a good qualitative agreement with LMRA results. The unfavorable interactions are compensated by various favorable interactions.

In summary we obtained very good results relating the variation of the 5-HT_{2B} receptor binding affinity with the variation of the value of several local atomic reactivity indices belonging to a common skeleton. Docking studies show a qualitative agreement with LMRA results. Two problems remain to be solved. The first one is related to the inclusion of substituents with different length in the common skeleton. The second one is the search of a more fine association between the results of both models.

REFERENCES

- [1] S Offermanns; W Rosenthal, *Encyclopedia of molecular pharmacology*, Springer, Berlin; New York, **2008**.
- [2] KD Tripathi, *Essentials of medical pharmacology*, Jaypee Brothers Medical Pub. 7 edition, New Delhi, **2013**.
- [3] NM Barnes; JF Neumaier, "Neuronal 5-HT Receptors and SERT," pp. 1-15, *Tocris Bioscience Scientific Review Series*, www.tocris.com, **2015**.
- [4] L Peng; L Gu; B Li; L Hertz, *Curr Neuropharmacol*, **2014**, 12, 365-379.
- [5] PM MacFarlane; S Vinit; GS Mitchell, *Neurosci.*, **2014**, 269, 67-78.
- [6] A Hunfeld; M Kremser; D Segelcke; H Lübbert, *J Headache Pain*, **2014**, 15, 1-1.
- [7] ME Gibbs; L Hertz, *Front. Pharmacol.*, **2014**, 5, 54.
- [8] S Bharti; N Rani; J Bhatia; D Arya, *Apoptosis*, **2014**, 1-11.
- [9] T Oshima; J Koseki; Y Nando; Z Li; T Kondo, et al., *Gastroenterol.*, **2013**, 144, S-544.
- [10] X Li; Y Ma; X Wu; Z Hao; J Yin, et al., *Biochem. Biophys. Res. Comm.*, **2013**, 441, 809-814.
- [11] DF Bilalova, *J. Electrocardiol.*, **2013**, 46, e7.
- [12] Z Aira; I Buesa; G García del Caño; J Bilbao; F Doñate, et al., *Pain*, **2013**, 154, 1865-1877.
- [13] N Urtikova; N Berson; J Van Steenwinckel; S Doly; J Truchetto, et al., *Pain*, **2012**, 153, 1320-1331.
- [14] SL Diaz; S Doly; N Narboux-Neme; S Fernandez; P Mazot, et al., *Mol Psychiatry*, **2012**, 17, 154-163.
- [15] C Cervantes-Durán; GC Vidal-Cantú; P Barragán-Iglesias; JB Pineda-Farias; M Bravo-Hernández, et al., *Pharmacol. Biochem. Behav.*, **2012**, 102, 30-35.
- [16] Z Aira; I Buesa; G García del Caño; M Salgueiro; N Mendiabre, et al., *Pain*, **2012**, 153, 1418-1425.
- [17] N Urtikova; J Van Steenwinckel; S Doly; L Maroteaux; M Pohl; M Conrath, *Eur. Neuropsychopharm.*, **2011**, 21, Supplement 3, S410-S411.
- [18] U Spampinato; A Cathala; F Panin; PV Piazza; AL Auclair, et al., *Eur. Neuropsychopharm.*, **2011**, 21, Supplement 3, S218.
- [19] K Ohashi-Doi; D Ferens; N Takahashi; K Kawamura; JB Furness, *Gastroenterol.*, **2011**, 140, S-611.
- [20] SL Diaz; L Maroteaux, *Neuropharmacol.*, **2011**, 61, 495-502.
- [21] S Diaz; S Doly; N Narboux-Nême; S Fernández; P Mazot; L Maroteaux, *Eur. Neuropsychopharm.*, **2011**, 21, Supplement 3, S218-S219.
- [22] L Bevilacqua; S Doly; J Kaprio; L Maroteaux; E Coccaro, et al., *Eur. Neuropsychopharm.*, **2011**, 21, Supplement 3, S218.
- [23] S Zhang; B Li; D Lovatt; J Xu; D Song, et al., *Neuron Glia Biol.*, **2010**, 6, 113-125.
- [24] B Svejda; M Kidd; F Giovino; K Eltawil; BI Gustafsson, et al., *Cancer*, **2010**, 116, 2902-2912.
- [25] H Nishio; T Hirai, *Neurosci. Res.*, **2010**, 68, Supplement 1, e224.
- [26] K Eltawil; B Svejda; F Giovino; A Timberlake; R Pfragner, et al., *Gastroenterol.*, **2010**, 138, S-25.
- [27] VS Tharayil; MM Wouters; JE Stanich; MD Gershon; L Maroteaux, et al., *Gastroenterol.*, **2009**, 136, A-51.
- [28] L Monassier; MA Laplante; P Bousquet; J De Champlain, *Arch. Cardiovasc. Dis.*, **2009**, 102, Supplement 1, S28.
- [29] M Wouters; VS Tharayil; JL Roeder; PR Strega; SJ Gibbons; G Farrugia, *Gastroenterol.*, **2008**, 134, A-102.
- [30] GJ Sanger; AK Bassil; VJ Bolton; CM Taylor; K Gray, et al., *Gastroenterol.*, **2008**, 134, A-543.
- [31] E Reisoli; S De Lucchini; T Anelli; S Biagioni; I Nardi; M Ori, *Brain. Res.*, **2008**, 1244, 32-39.
- [32] MM Wouters; SJ Gibbons; JL Roeder; M Distad; Y Ou, et al., *Gastroenterol.*, **2007**, 133, 897-906.
- [33] M Locker; J Bitard; C Collet; A Poliard; V Mutel, et al., *Cell. Sign.*, **2006**, 18, 628-639.
- [34] A Fabre; J Marchai; S Marchand-Adam; C Ruffie; J Callebort, et al., *Revue Malad. Respir.*, **2005**, 22, 849.
- [35] R Lawson; B Gasser; E Ayme-Dietrich; L Maroteaux; L Monassier, *Arch. Cardiovasc. Dis. Supp.*, **2014**, 6, Supplement 1, 72.
- [36] I Cavero; J-M Guillon, *J. Pharm. Exper. Ther.*, **2014**, 69, 150-161.
- [37] E Ayme-Dietrich; B Gasser; R Lawson; J-P Mazzucotelli; L Monassier, *Arch. Cardiovasc. Dis. Supp.*, **2014**, 6, Supplement 1, 73.
- [38] CS Elangbam; LE Job; LM Zadrozny; JC Barton; LW Yoon, et al., *Exp. Toxicol. Pathol.*, **2008**, 60, 253-262.

- [39] KP Latté; T Görnemann; B Schurad; HH Pertz, *Parkinson. Relat. Dis.*, **2007**, 13, Supplement 2, S120-S121.
- [40] S Ponnala; N Kapadia; WW Harding, *MedChemComm*, **2015**, DOI: 10.1039/C4MD00418C.
- [41] DA Williams; SA Zaidi; Y Zhang, *Bioorg. Med. Chem. Lett.*, **2014**, 24, 1489-1492.
- [42] T Rodrigues; N Hauser; D Reker; M Reutlinger; T Wunderlin, et al., *Ang. Chem.*, **2014**, DOI: 10.1002/anie.201410201.
- [43] CE Canal; D Morgan; D Felsing; K Kondabolu; NE Rowland, et al., *J. Pharm. Exptl. Ther.*, **2014**, 349, 310-318.
- [44] PI Dosa; T Ward; MA Walters; SW Kim, *ACS Med. Chem. Lett.*, **2013**, 4, 254-258.
- [45] N Takahashi; K Inagaki; K Taniguchi; Y Sakaguchi; K Kawamura, *Gastroenterol.*, **2011**, 140, S-607.
- [46] G Szenasi, *Eur. Neuropsychopharm.*, **2011**, 21, Supplement 3, S218.
- [47] M Hansen, "Design and Synthesis of Selective Serotonin Receptor Agonists for Positron Emission Tomography Imaging of the Brain," *Faculty of Pharmaceutical Sciences*, PhD Thesis, pp. 227, University of Copenhagen, Copenhagen, **2010**.
- [48] H Bienaymé; L Chêne; S Grisoni; A Grondin; E-B Kaloun, et al., *Bioorg. Med. Chem. Lett.*, **2006**, 16, 4830-4833.
- [49] R Borman; A Oxford; S Denny; A Sykes; S Samra, et al., *Gastroenterol.*, **2003**, 124, A569.
- [50] JE Audia; DA Evrard; GR Murdoch; JJ Droste; JS Nissen, et al., *J. Med. Chem.*, **1996**, 39, 2773-2780.
- [51] IT Forbes; GE Jones; OE Murphy; V Holland; GS Baxter, *J. Med. Chem.*, **1995**, 38, 855-857.
- [52] IT Forbes; P Ham; DH Booth; RT Martin; M Thompson, et al., *J. Med. Chem.*, **1995**, 38, 2524-2530.
- [53] D Wacker; C Wang; V Katritch; GW Han; X-P Huang, et al., *Science*, **2013**, 340, 615-619.
- [54] YC Martin, *Quantitative drug design: a critical introduction*, M. Dekker, New York, **1978**.
- [55] JS Gómez-Jeria, *Int. J. Quant. Chem.*, **1983**, 23, 1969-1972.
- [56] JS Gómez-Jeria, "Modeling the Drug-Receptor Interaction in Quantum Pharmacology," in *Molecules in Physics, Chemistry, and Biology*, J. Maruani Ed., vol. 4, pp. 215-231, Springer Netherlands, **1989**.
- [57] JS Gómez-Jeria; M Ojeda-Vergara, *J. Chil. Chem. Soc.*, **2003**, 48, 119-124.
- [58] JS Gómez-Jeria, *Elements of Molecular Electronic Pharmacology (in Spanish)*, Ediciones Sokar, Santiago de Chile, **2013**.
- [59] JS Gómez-Jeria, *Canad. Chem. Trans.*, **2013**, 1, 25-55.
- [60] K Fukui; H Fujimoto, *Frontier orbitals and reaction paths: selected papers of Kenichi Fukui*, World Scientific, Singapore; River Edge, N.J., **1997**.
- [61] JS Gómez-Jeria; L Espinoza, *Bol. Soc. Chil. Quím.*, **1982**, 27, 142-144.
- [62] JS Gómez-Jeria; D Morales-Lagos, "The mode of binding of phenylalkylamines to the Serotonergic Receptor," in *QSAR in design of Bioactive Drugs*, M. Kuchar Ed., pp. 145-173, Prous, J.R., Barcelona, Spain, **1984**.
- [63] JS Gómez-Jeria; DR Morales-Lagos, *J. Pharm. Sci.*, **1984**, 73, 1725-1728.
- [64] JS Gómez-Jeria; D Morales-Lagos; JI Rodríguez-Gatica; JC Saavedra-Aguilar, *Int. J. Quant. Chem.*, **1985**, 28, 421-428.
- [65] JS Gómez-Jeria; D Morales-Lagos; BK Cassels; JC Saavedra-Aguilar, *Quant. Struct.-Relat.*, **1986**, 5, 153-157.
- [66] JS Gómez-Jeria; BK Cassels; JC Saavedra-Aguilar, *Eur. J. Med. Chem.*, **1987**, 22, 433-437.
- [67] JS Gómez-Jeria; P Sotomayor, *J. Mol. Struct. (Theochem)*, **1988**, 166, 493-498.
- [68] JS Gómez-Jeria; M Ojeda-Vergara; C Donoso-Espinoza, *Mol. Engn.*, **1995**, 5, 391-401.
- [69] JS Gómez-Jeria; L Lagos-Arancibia, *Int. J. Quant. Chem.*, **1999**, 71, 505-511.
- [70] JS Gómez-Jeria; L Lagos-Arancibia; E Sobarzo-Sánchez, *Bol. Soc. Chil. Quím.*, **2003**, 48, 61-66.
- [71] JS Gómez-Jeria; F Soto-Morales; G Larenas-Gutierrez, *Ir. Int. J. Sci.*, **2003**, 4, 151-164.
- [72] JS Gómez-Jeria; LA Gerli-Candia; SM Hurtado, *J. Chil. Chem. Soc.*, **2004**, 49, 307-312.
- [73] F Soto-Morales; JS Gómez-Jeria, *J. Chil. Chem. Soc.*, **2007**, 52, 1214-1219.
- [74] JS Gómez-Jeria; F Soto-Morales; J Rivas; A Sotomayor, *J. Chil. Chem. Soc.*, **2008**, 53, 1393-1399.
- [75] JS Gómez-Jeria, *J. Chil. Chem. Soc.*, **2010**, 55, 381-384.
- [76] T Bruna-Larenas; JS Gómez-Jeria, *Int. J. Med. Chem.*, **2012**, 2012 Article ID 682495, 1-16.
- [77] JS Gómez-Jeria, *Der Pharm. Lett.*, **2014**, 6., 95-104.
- [78] JS Gómez-Jeria, *SOP Trans. Phys. Chem.*, **2014**, 1, 10-28.
- [79] JS Gómez-Jeria, *Res. J. Pharmac. Biol. Chem. Sci.*, **2014**, 5, 2124-2142.
- [80] JS Gómez-Jeria, *J. Comput. Methods Drug Des.*, **2014**, 4, 32-44.
- [81] JS Gómez-Jeria, *Res. J. Pharmac. Biol. Chem. Sci.*, **2014**, 5, 424-436.
- [82] JS Gómez-Jeria, *Res. J. Pharmac. Biol. Chem. Sci.*, **2014**, 5, 780-792.
- [83] JS Gómez-Jeria; J Molina-Hidalgo, *J. Comput. Methods Drug Des.*, **2014**, 4, 1-9.
- [84] JS Gómez-Jeria; J Valdebenito-Gamboa, *Der Pharma Chem.*, **2014**, 6, 383-406.
- [85] F Salgado-Valdés; JS Gómez-Jeria, *J. Quant. Chem.*, **2014**, 2014 Article ID 431432, 1-15.
- [86] R Solís-Gutiérrez; JS Gómez-Jeria, *Res. J. Pharmac. Biol. Chem. Sci.*, **2014**, 5, 1401-1416.
- [87] MS Leal; A Robles-Navarro; JS Gómez-Jeria, *Der Pharm. Lett.*, **2015**, 7, 54-66.

- [88] C Barahona-Urbina; S Nuñez-Gonzalez; JS Gómez-Jeria, *J. Chil. Chem. Soc.*, **2012**, 57, 1497-1503.
- [89] DA Alarcón; F Gatica-Díaz; JS Gómez-Jeria, *J. Chil. Chem. Soc.*, **2013**, 58, 1651-1659.
- [90] JS Gómez-Jeria; M Flores-Catalán, *Canad. Chem. Trans.*, **2013**, 1, 215-237.
- [91] A Paz de la Vega; DA Alarcón; JS Gómez-Jeria, *J. Chil. Chem. Soc.*, **2013**, 58, 1842-1851.
- [92] I Reyes-Díaz; JS Gómez-Jeria, *J. Comput. Methods Drug Des.*, **2013**, 3, 11-21.
- [93] F Gatica-Díaz; JS Gómez-Jeria, *J. Comput. Methods Drug Des.*, **2014**, 4, 79-120.
- [94] JS Gómez-Jeria, *Int. Res. J. Pure App. Chem.*, **2014**, 4, 270-291.
- [95] JS Gómez-Jeria, *Brit. Microbiol. Res. J.*, **2014**, 4, 968-987.
- [96] JS Gómez-Jeria, *Der Pharma Chem.*, **2014**, 6, 64-77.
- [97] JS Gómez-Jeria, *J. Comput. Methods Drug Des.*, **2014**, 4, 38-47.
- [98] D Muñoz-Gacitúa; JS Gómez-Jeria, *J. Comput. Methods Drug Des.*, **2014**, 4, 33-47.
- [99] D Muñoz-Gacitúa; JS Gómez-Jeria, *J. Comput. Methods Drug Des.*, **2014**, 4, 48-63.
- [100] DI Pino-Ramírez; JS Gómez-Jeria, *Amer. Chem. Sci. J.*, **2014**, 4, 554-575.
- [101] JS Gómez-Jeria; A Robles-Navarro, *Res. J. Pharmac. Biol. Chem. Sci.*, **2015**, 6, 1337-1351.
- [102] MJ Frisch; GW Trucks; HB Schlegel; GE Scuseria; MA Robb, et al., Gaussian98 Rev. A.11.3, Gaussian, Pittsburgh, PA, USA, **2002**.
- [103] JS Gómez-Jeria, D-Cent-QSAR: A program to generate Local Atomic Reactivity Indices from Gaussian log files. 1.0, Santiago, Chile, **2014**.
- [104] JS Gómez-Jeria, *J. Chil. Chem. Soc.*, **2009**, 54, 482-485.
- [105] O Trott; AJ Olson, *J. Comput. Chem.*, **2010**, 31, 455-461.
- [106] Accelrys Software Inc., Discovery Studio Visualizer 4.0, Accelrys Software Inc., San Diego, CA, USA, **2013**.
- [107] GM Morris; R Huey; AJ Olson, "Using AutoDock for Ligand-Receptor Docking," in *Current Protocols in Bioinformatics*, John Wiley & Sons, Inc., **2002**.